Table 1. Characteristics of HCC Cases and Controls

Study Variables	HCC Cases: Number with Complete Data	HCC Cases: n (%)	Controls: Number with Complete Data	Controls: n (%)
Matched variables				
Gender	224		644	
Male		136 (60.7)		387 (60.1)
Female		88 (39.3)		257 (39.9)
Age at HCC diagnosis (yr)	224	67.6 (10.1)*	–	–
City	224		644	
Hiroshima		155 (69,2)		444 (68.9)
Nagasaki		69 (30.8)		200 (31.1)
Age at serum storage (yr)	224	66.4 (10.2)*	644	63.7 (9.8)*
Unmatched variables				
Viral etiology	211		640	
HBV−/HCV −		45 (21.3)		579 (90.5)
HBV+/HCV −		29 (13.7)		18 (2.8)
HBV−/HCV +		132 (62.6)		41 (6.4)
HBV +/HCV +		5 (2.4)		2 (0.3)
Alcohol consumption (g ethanol/day)	199		577	
None		97 (48.7)		315 (54.6)
0< <20		37 (18.6)		130 (22.5)
20≤ <40		20 (10.1)		64 (11.1)
≥40		45 (22.6)		68 (11.8)
BMI (kg/m^2)	210		633	
10 yrs before diagnosis				
≤19.5		38 (18.1)		122 (19.3)
19.6 - 21.2		33 (15.7)		136 (21.5)
21.3 - 22.9		36 (17.2)		142 (22.4)
23.0 - 25.0		49 (23.3)		124 (19.6)
>25.0		54 (25.7)		109 (17.2)
Smoking habit	199		578	
Never		80 (40.2)		283 (49.0)
Current smoker		107 (53.8)		262 (45.3)
Former smoker		12 (6.0)		33 (5.7)
Radiation dose to the liver (Gy)	204	0.46 (0.69)*	606	0.34 (0.56)*,†

*Mean (SD).
†Weighted mean radiation dose (among controls), calculated by weighting according to their countermatching selection probabilities.

BMI, and smoking habit based on all cases of HCC. The analysis was performed using 186 HCC cases and 600 controls, both separately (radiation only or hepatitis virus infection only) and jointly (radiation and hepatitis virus infection were fit simultaneously), based on subjects with known radiation dose and known HBV and HCV infection status. In analyses where effects of radiation and hepatitis virus infection were fitted separately, unadjusted RR at 1 Gy of HCC for radiation was 1.40 (95% confidence interval [CI], 1.07-1.89, $P = 0.013$), whereas unadjusted RRs of HCC for HBV+/HCV− status and HBV−/HCV+ status were 34 (95% CI, 13-106, $P < 0.001$) and 57 (95% CI, 27-140, $P < 0.001$), respectively. After adjustment for categorical alcohol consumption, BMI, and smoking habit, significant association was found between HCC and radiation dose or hepatitis virus infection, resulting in an RR at 1 Gy of 1.67 (95% CI, 1.22-2.35, $P < 0.001$) for radiation and RRs of 63 (95% CI, 20-241, $P < 0.001$) for HBV+/HCV− status and 83 (95% CI, 36-231, $P < 0.001$) for HBV−/HCV+ status. The above estimates changed little when radiation and hepatitis virus infection were fit simultaneously.

Risk of HCC for Radiation After Excluding Persons with Either or Both Hepatitis Virus Infections. After excluding subjects with either or both hepatitis virus infections, the RRs at 1 Gy of HCC for radiation were estimated as shown in Table 3. There were 161 cases including 119 HCV-infected individuals and 452 matched controls including 29 HCV-infected individuals without HBV infection only. There were 66 cases including 24 HBV-infected individuals and 176 matched controls including 5 HBV-infected individuals without HCV infection only. The adjusted analyses indicated that radiation exposure was significantly associated with increased risks for HCC,

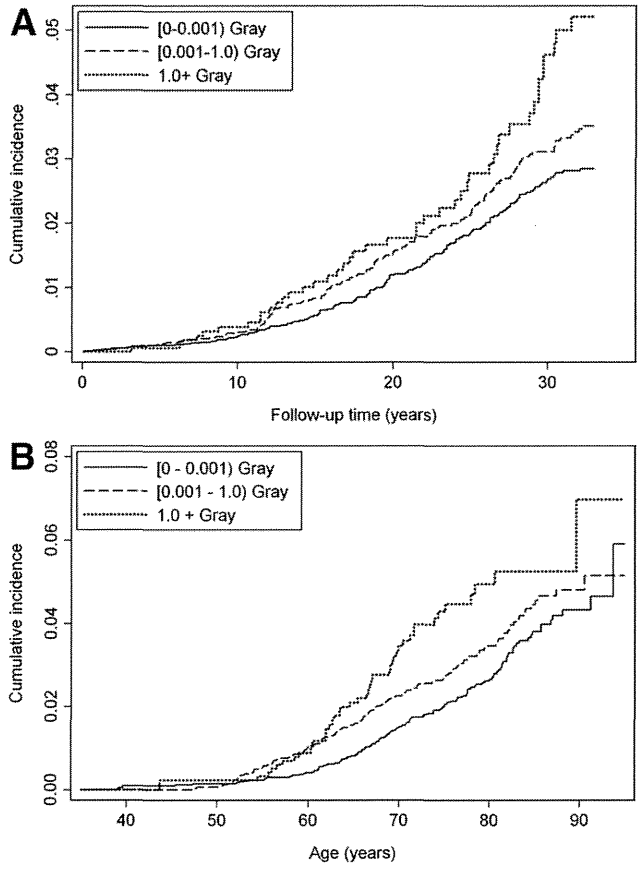

Fig. 1. Cumulative incidence of HCC (1970-2002) by radiation dose. Dotted line: radiation dose ≥1.0 Gy; dashed line: radiation dose 0.001 ≤ <1.0 Gy; solid line, radiation dose 0 ≤ <0.001 Gy. Cumulative HCC incidence by follow-up time (A) and age (B) increased significantly ($P = 0.028$, $P = 0.0003$, respectively) with radiation dose.

even after excluding HBV- or HCV-infected individuals. Furthermore, significant association was found between non-B, non-C HCC and radiation dose, resulting in an RR at 1 Gy of 1.90 (95% CI, 1.02-3.92, $P = 0.041$) for radiation without adjustment for categorical alcohol consumption, BMI, and smoking habit and 2.74 (95% CI, 1.26-7.04, $P = 0.007$) with such adjustment.

Risk of Non-B, Non-C HCC. Effects of alcohol consumption, BMI, and smoking habit on non-B, non-C HCC risk with or without adjustment for radiation dose were estimated using continuous and categorical covariates as shown in Table 4. RRs for continuous covariates are for a one-unit difference in the factor. Risk of non-B, non-C HCC for alcohol consumption per 20 g of ethanol per day was significant with a log-linear model (adjusted RR 1.64, 95% CI, 1.05-2.81, $P = 0.029$), but was limited to the category ≥40 g of ethanol per day (adjusted RR 5.49, 95% CI, 0.98-39.2, $P = 0.052$). Significant log-linear association was not found with continuous BMI, and even the category BMI >25.0 kg/m^2 (obese) 10 years before diagnosis did not evidence significant risk despite a rather large estimate of RR (adjusted RR 3.17, 95% CI, 0.92-12.3, $P = 0.068$). Current smoking evidenced significant risk (adjusted RR 5.95, 95% CI, 1.34-33.2, $P = 0.018$), but there were no continuous data on amount smoked. These results indicate that alcohol consumption per 20 g of ethanol per day, current smoking, and perhaps BMI of >25.0 kg/m^2 10 years before diagnosis are associated independently with increased risk for non-B, non-C HCC.

Discussion

The present study confirmed that radiation is associated with increased incidence of HCC among atomic bomb survivors. Additionally, the nested case-control study indicates that radiation and HBV and HCV infection are associated with increased risk for HCC, and that radiation remains an independent risk factor for HCC after taking into account hepatitis virus infection, alcohol consumption, BMI 10 years before HCC diagnosis, and smoking habit. Furthermore, significant association was observed between non-B, non-C HCC and radiation dose, alcohol consumption, and smoking, whereas obesity 10 years before diagnosis was marginally significantly associated with increased risk for non-B, non-C HCC.

In the analysis (Table 2) in which radiation dose and hepatitis virus infection were fitted separately, radiation was significantly associated with increased risk

Table 2. Risk of HCC for Radiation and HBV or HCV Infection Status

Variables	Number of Cases/Controls	Unadjusted RR (95% CI)		Adjusted* RR (95%CI)	
		Alone†	Joint‡	Alone†	Joint‡
Radiation (at 1Gy)	186/600	1.40 (1.07-1.89)	1.39 (0.93-2.26)	1.67 (1.22-2.35)	1.82 (1.09-3.34)
HBV+/HCV −	24/14	34 (13-106)	30 (11-91)	63 (20-241)	50 (16-184)
HBV−/HCV +	119/35	57 (27-140)	58 (28-147)	83 (36-231)	87 (37-251)

Abbreviations: CI, confidence interval; RR, relative risk.

*Adjusted for categorical alcohol consumption, BMI 10 yrs before diagnosis, and smoking habit.

†Radiation dose to the liver and hepatitis virus infection status were fit separately.

‡Radiation dose to the liver and hepatitis virus infection status were fit simultaneously.

Table 3. Risk of HCC for Radiation After Excluding Persons Infected with HBV and/or HCV

Subjects	Number of Cases/Controls	Unadjusted RR at 1 Gy (95% CI)	Adjusted* RR at 1 Gy (95% CI)
Exclude HBV+ (no HCV adjustment)	161/452	1.48 (1.10-2.05)	1.91 (1.34-2.81)
(adjust for HCV)		1.60 (0.997-2.78)	2.32 (1.25-4.76)
Exclude HCV+ (no HBV adjustment)	66/176	1.61 (1.003-2.76)	1.91 (1.13-3.48)
(adjust for HBV)		1.68 (0.96-3.23)	2.16 (1.12-4.76)
Exclude both HBV+ and HCV+†	42/108	1.90 (1.02-3.92)	2.74 (1.26-7.04)

Abbreviations: CI, confidence interval; RR, relative risk.
*Adjusted for categorical alcohol consumption, BMI 10 yrs before diagnosis, and smoking habit.
†Non-B, non-C status.

for HCC with or without adjustment for alcohol consumption, BMI, and smoking habit. Although this finding is in agreement with our previous understanding that liver cancer risk is significantly associated with radiation without adjustment for hepatitis virus infection among atomic bomb survivors, it is difficult to compare the HCC risk estimates between the previous and current study results.[13-16] The difficulty is caused by the inclusion of hepatoblastoma and intrahepatic cholangiocarcinoma in addition to HCC as liver cancer cases in analyses of tumor registry-based liver cancer risk (ERR at 1 Sv = 0.49),[13] mortality study- and tumor registry-based[15,16] liver cancer mortality risk (male: ERR per Sv = 0.39, female: ERR per Sv = 0.35), and liver cancer risk (male: ERR per Gy = 0.32, female: ERR per Gy = 0.28), despite the fact that the majority of liver cancer cases were HCC. Because a relatively large fraction of liver cancer cases was included that were diagnosed only on the basis of death certificates,[13,16] complete exclusion of metastatic liver tumor cases from such cases may not have been possible. Metastatic liver tumor cases were excluded in an analysis of pathological review-based liver cancer risk (ERR per Gy = 0.81), but hepatoblastoma and intrahepatic cholangiocarcinoma were included with HCC.[14]

In the current analyses adjusted for alcohol consumption, BMI, and smoking habit, the RR estimates for radiation increased slightly and showed statistical significance with adjustment for HBV and HCV infection status. HBV infection may be considered an intermediate risk factor for HCC, because three of four previous HBV screenings demonstrated that HBsAg prevalence increases with radiation dose[17-19,38]; therefore, adjustment for HBV infection status might be expected to result in a decreased radiation risk estimate. However, such interpretation is difficult because

Table 4. Risk of Non-B, Non-C HCC for Alcohol Consumption, BMI, and Smoking Habit

Variables	Number of Cases/Controls	Unadjusted RR (95% CI)†	Adjusted* RR (95% CI)†
Continuous			
Alcohol consumption (per 20 g ethanol per day)	37/96	1.51 (0.98-2.60)	1.64 (1.05-2.81)
BMI 10 yrs before diagnosis (per +1 kg/m^2 difference)	41/107	1.06 (0.95-1.18)	1.06 (0.95-1.19)
Categorical			
Alcohol consumption (g ethanol per day)			
None	22/58	1	1
0 < < 20	5/21	0.98 (0.24-3.60)	0.85 (0.18-3.48)
20 ≤ < 40	2/10	0.78 (0.09-4.49)	0.68 (0.08-4.07)
≥ 40	8/7	5.25 (1.04-33.5)	5.49 (0.98-39.2)
BMI (kg/m^2) 10 yrs before diagnosis			
≤ 19.5	8/18	1.64 (0.45-6.20)	1.66 (0.42-6.83)
19.6 - 21.2	3/22	0.74 (0.12-3.66)	0.80 (0.13-4.15)
21.3 - 22.9	6/25	1	1
23.0 - 25.0	10/24	1.76 (0.42-7.93)	2.37 (0.52-11.5)
> 25.0	14 /18	2.85 (0.86-10.5)	3.17 (0.92-12.3)
Smoking habit			
Never	17/58	1	1
Current smoker	19/38	3.78 (0.99-17.1)	5.95 (1.34-33.2)
Former smoker	1/3	2.83 (0.10-52.3)	4.67 (0.16-93.7)

Abbreviations: CI, confidence interval; RR, relative risk.
*Adjusted for radiation dose to the liver.
†Alcohol consumption, BMI, and smoking habit were fit simultaneously, either as continuous (alcohol and BMI only) or categorical factors.

the risk estimate was also adjusted for HCV infection status, although anti-HCV Ab prevalence is not significantly associated with radiation dose.[20] We therefore examined HBV and HCV infection status and concomitant radiation effects separately, excluding persons with one or the other viral infection.

RRs of HCC for radiation after excluding persons infected with HBV or HCV were generally higher than with the full data, but differed little depending on which virus was used for exclusion (Table 3). As with the full data, adjustment for HBV or HCV infection status reduced the statistical significance of the radiation effect but had little impact on the RR estimates themselves. The RR of HCC for radiation after excluding persons infected with HBV and HCV (i.e., the RR of non-B, non-C HCC for radiation) was significant with or without adjustment for alcohol consumption, BMI, and smoking habit. As there can be no viral mediation of the radiation risk in noninfected individuals, lower radiation risks estimated in infected individuals might be considered evidence of mediation, but mediation would imply that risk decreases with adjustment for viral infection status, which did not occur. The reduction in statistical significance with adjustment for HBV and HCV infection status might be due to loss of power when further parameters for the risks of HCC for hepatitis virus infection are estimated or the number of subjects is reduced by exclusion.

As with the results reported previously,[1] there is evidence that alcohol consumption of $\geq$40 g/day ethanol and BMI >25.0 kg/m^2 10 years before diagnosis are associated with non-B, non-C HCC risk (Table 4). However, the evidence is not as strong given the small amount of data after excluding persons infected with HBV and HCV. The current study demonstrates that smoking is significantly associated with non-B, non-C HCC risk, although lack of continuous data precluded estimation of the relationship to amount smoked. This finding is consistent with recent assessments by the International Agency for Research on Cancer (IARC) where HCC has been positioned as a smoking-related malignant disease.[39] Some studies have shown effects of smoking on risk of HCC, but few studies have incorporated, in a strict and in-depth manner, HBV and HCV infections.[11,40]

Cohort studies of atomic bomb survivors[13-16] and Mayak nuclear facility workers[22-24] have indicated beyond a doubt that radiation increases liver cancer risk, even though hepatitis virus infection was not taken into account. It is also well known that persistent long-term internal exposure to α particles from Thorotrast, a radioactive contrast agent, can induce hemangiosarcoma, cholangiocarcinoma, and HCC in humans.[41-43] Because a significant radiation effect is observed in a high proportion of HCC cases having a p53 mutation, it has been suggested that p53 is one of the intracellular targets of atomic bomb radiation and thus a cause of the increased HCC incidence among atomic bomb survivors.[44] A lifespan study in mice exposed to continuous low-dose-rate γ rays demonstrated that the incidence of HCC was significantly increased, especially in male mice.[25] Liver weights of irradiated mice were significantly greater than those of nonirradiated controls, and the lipid content was significantly increased in irradiated mouse livers.[45] It is considered that hepatic steatosis itself is a state conferring risk for high carcinogenicity, and that in steatohepatitis, oxidative stress due to fatty acid oxidation in hepatocytes may cause DNA injury and eventually lead to carcinogenesis.[46] There is a significant association of radiation dose with prevalence of fatty liver among Nagasaki AHS participants, although a significant association has not been found between obesity (BMI $\geq$26.0 kg/m^2) and radiation dose.[47] These findings may explain part of the mechanism of increased risks of HCC with radiation exposure.

The main strengths of our study include its prospective cohort-based, nested case-control design, which minimizes selection bias, the use of stored sera, and a wealth of epidemiological information obtained prior to HCC diagnosis. It is difficult and expensive to perform full cohort serum analyses, whereas the nested case-control design utilized here can provide substantial reductions in cost and effort with little loss of statistical efficiency.[36] Another major strength of our study is that it incorporated, in a strict and in-depth manner, hepatitis virus infection status and HCC cases were identified through the Hiroshima Tumor and Tissue Registry and Nagasaki Cancer Registry, supplemented by additional cases detected by way of pathological review of related diseases.[26]

A limitation of our study is that the joint effects of radiation and hepatitis virus infection could not be estimated from the standpoint of causality. As discussed previously, HBV and possibly HCV infection may act as intermediate risk factors in radiation-associated HCC. Previous studies have consistently demonstrated that prevalence of HBsAg increases with radiation dose within the AHS,[17-19] although no dose response for anti-HCV Ab has been detected.[20] Therefore, when the risk of HCC for radiation is estimated while controlling for HBV infection, some of the radiation risk may be absorbed in the coefficient for HBV infection. In other words, the radiation risk coefficient

does not represent the radiation effect independent of mediation by HBV infection and the HCC risk for HBV infection itself is not correctly estimated, because the actual causal pathway is not explicitly modeled. In addition, we cannot easily disentangle the joint effects of radiation and HBV infection using standard regression models, because HBV infection is not a true confounding risk factor but an intermediate risk factor. Nevertheless, that the radiation risk did not decrease with concomitant adjustment for viral infection suggests that the practical extent of mediation may be small. We are currently developing methods of statistical analysis that jointly consider the dose response for the intermediate viral factor as well as the joint risk of HCC for both hepatitis virus infection and radiation in the countermatched, nested case-control design.

In conclusion, radiation exposure was associated with increased risk of HCC, even after adjusting for HBV or HCV infection, alcohol consumption, BMI, and smoking habit. Moreover, radiation exposure was an independent risk factor for non-B, non-C HCC with no apparent confounding by alcohol consumption, BMI, or smoking habit. The mechanistic form of joint effects of radiation and HBV or HCV infection on HCC risk could not be estimated, but the development of new statistical methods that jointly consider the dose response for the intermediate viral factor will make such an analysis possible in the future. In particular, in-depth understanding of the mechanisms by which radiation exposure as well as obesity, alcohol drinking, and smoking contribute to development of non-B, non-C HCC may lead to prevention, early detection, and better therapeutic strategies.

Acknowledgment: We thank Naomi Masunari and Sachiyo Funamoto for the collection and processing of the data and all members of the Division of Clinical Laboratories for excellent assistance. The RERF, Hiroshima and Nagasaki, Japan is a private, nonprofit foundation funded by the Japanese Ministry of Health, Labour and Welfare (MHLW) and the U.S. Department of Energy (DOE), the latter in part through the National Academy of Sciences. This publication was supported by RERF Research Protocol(s) 2-75 and 1-04.

References

1. Ohishi W, Fujiwara S, Cologne JB, Suzuki G, Akahoshi M, Nishi N, et al. Risk factors for hepatocellular carcinoma in a Japanese population: a nested case-control study. Cancer Epidemiol Biomar 2008;17:846-854.
2. Umemura T, Kiyosawa K. Epidemiology of hepatocellular carcinoma in Japan. Hepatol Res 2007;37:S95-S100.
3. Abe H, Yoshizawa K, Kitahara T, Aizawa R, Matsuoka M, Aizawa Y. Etiology of non-B, non-C hepatocellular carcinoma in the eastern district of Tokyo. J Gastroenterol 2008;43:967-974.
4. Marrero JA, Fontana RJ, Su GL, Conjeevaram HS, Emick DM, Lok AS. NAFLD may be a common underlying liver disease in patients with hepatocellular carcinoma in the United States. HEPATOLOGY 2002; 36:1349-1354.
5. Niederau C, Fischer R, Pürschel A, Stremmel W, Häussinger D, Strohmeyer G. Long-term survival in patients with hereditary hemochromatosis. Gastroenterology 1996;110:1107-1119.
6. Yoshiike N, Lwin H. Epidemiological aspects of obesity and NASH/NAFLD in Japan. Hepatol Res 2005;33:77-82.
7. Gupta K, Krishnaswamy G, Karnad A, Peiris AN. Insulin: a novel factor in carcinogenesis. Am J Med Sci 2002;323:140-145.
8. El-Serag HB, Tran T, Everhart JE. Diabetes increases the risk of chronic liver disease and hepatocellular carcinoma. Gastroenterology 2004;126:460-468.
9. Inoue M, Iwasaki M, Otani T, Sasazuki S, Noda M, Tsugane S. Diabetes mellitus and the risk of cancer: results from a large-scale population-based cohort study in Japan. Arch Intern Med 2006;166:1871-1877.
10. Caldwell SH, Crespo DM, Kang HS, Al-Osaimi AM. Obesity and hepatocellular carcinoma. Gastroenterology 2004;127:S97-103.
11. Marrero JA, Fontana RJ, Fu S, Conjeevaram HS, Su GL, Lok AS. Alcohol, tobacco and obesity are synergistic risk factors for hepatocellular carcinoma. J Hepatol 2005;42:218-224.
12. Saunders D, Seidel D, Allison M, Lyratzopoulos G. Systematic review: the association between obesity and hepatocellular carcinoma — epidemiological evidence. Aliment Pharmacol Ther 2010;31:1051-63.
13. Thompson DE, Mabuchi K, Ron E, Soda M, Tokunaga M, Ochikubo S, et al. Cancer incidence in atomic bomb survivors. Part II: Solid tumors, 1958-1987. Radiat Res 1994;137:S17-67.
14. Cologne JB, Tokuoka S, Beebe GW, Fukuhara T, Mabuchi K. Effects of radiation on incidence of primary liver cancer among atomic bomb survivors. Radiat Res 1999;152:364-373.
15. Preston DL, Shimizu Y, Pierce DA, Suyama A, Mabuchi K. Studies of mortality of atomic bomb survivors. Report 13: solid cancer and noncancer disease mortality: 1950-1997. Radiat Res 2003;160:381-407.
16. Preston DL, Ron E, Tokuoka S, Funamoto S, Nishi N, Soda M, et al. Solid cancer incidence in atomic bomb survivors: 1958-1998. Radiat Res 2007;168:1-64.
17. Kato H, Mayumi M, Nishioka K, Hamilton HB. The relationship of hepatitis B surface antigen and antibody to atomic-bomb radiation in the Adult Health Study sample, 1975-1977. Am J Epidemiol 1983; 117:610-620.
18. Neriishi K, Akiba S, Amano T, Ogino T, Kodama K. Prevalence of hepatitis B surface antigen, hepatitis B e antigen and antibody, and antigen subtypes in atomic-bomb survivors. Radiat Res 1995;144:215-221.
19. Fujiwara S, Sharp GB, Cologne JB, Kusumi S, Akahoshi M, Kodama K, et al. Prevalence of hepatitis B virus infection among atomic bomb survivors. Radiat Res 2003;159:780-786.
20. Fujiwara S, Kusumi S, Cologne J, Akahoshi M, Kodama K, Yoshizawa H. Prevalence of anti-hepatitis C virus antibody and chronic liver disease among atomic bomb survivors. Radiat Res 2000;154:12-19.
21. Sharp GB, Mizuno T, Cologne JB, Fukuhara T, Fujiwara S, Tokuoka S, et al. Hepatocellular carcinoma among atomic bomb survivors: significant interaction of radiation with hepatitis C virus infections. Int J Cancer 2003;103:531-537.
22. Gilbert ES, Koshurnikova NA, Sokolnikov M, Khokhryakov VF, Miller S, Preston DL, et al. Liver cancers in Mayak workers. Radiat Res 2000; 154:246-252.
23. Tokarskaya ZB, Zhuntova GV, Scott BR, Khokhryakov VF, Belyaeva ZD, Vasilenko EK, et al. Influence of alpha and gamma radiations and non-radiation risk factors on the incidence of malignant liver tumors among Mayak PA workers. Health Phys 2006;91:296-310.
24. Sokolnikov ME, Gilbert ES, Preston DL, Ron E, Shilnikova NS, Khokhryakov VV, et al. Lung, liver and bone cancer mortality in Mayak workers. Int J Cancer 2008;123:905-911.
25. Tanaka IB 3rd, Tanaka S, Ichinohe K, Matsushita S, Matsumoto T, Otsu H, et al. Cause of death and neoplasia in mice continuously exposed to very low dose rates of gamma rays. Radiat Res 2007;167:417-437.26.

26. Fukuhara T, Sharp GB, Mizuno T, Itakura H, Yamamoto M, Tokunaga M, et al. Liver cancer in atomic-bomb survivors: histological characteristics and relationships to radiation and hepatitis B and C viruses. J Radiat Res 2001;42:117-130.
27. Cologne JB, Sharp GB, Neriishi K, Verkasalo PK, Land CE, Nakachi K. Improving the efficiency of nested case-control studies of interaction by selecting controls using counter matching on exposure. Int J Epidemiol 2004;33:485-492.
28. Ohishi W, Fujiwara S, Suzuki G, Kishi T, Sora M, Matsuura S, et al. Feasibility of freeze-dried sera for serological and molecular biological detection of hepatitis B and C viruses. J Clin Microbiol 2006;44: 4593-4595.
29. Ohishi W, Fujiwara S, Suzuki G, Chayama K. Validation of the use of freeze-dried sera for the diagnosis of hepatitis B and C virus infections in a longitudinal study cohort. In: Mohan RM, ed. Research Advances in Microbiology 7. Kerala, India: Global Research Network; 2007:1-9.
30. Young RW, Kerr GD, editors. Reassessment of the Atomic Bomb Radiation Dosimetry for Hiroshima and Nagasaki, Dosimetry System 2002, Report of the Joint US-Japan Working Group. Hiroshima, Japan: Radiation Effects Research Foundation; 2005.
31. Sharp GB, Lagarde F, Mizuno T, Sauvaget C, Fukuhara T, Allen N, et al. Relationship of hepatocellular carcinoma to soya food consumption: a cohort-based, case-control study in Japan. Int J Cancer 2005; 115:290-295.
32. The World Health Organization Western Pacific Region; The International Association for the Study; The International Obesity Task Force. The Asia-Pacific Perspective: Redefining Obesity and Its Treatment. Sydney, Australia: Health Communications Australia Pty Limited; 2000.
33. Langholz B, Borgan Ø. Counter-matching: a stratified nested case-control sampling method. Biometrika 1985;82:69-79.
34. Breslow NE, Day NE. Statistical Methods in Cancer Research: Volume 1—The Analysis of Case-control Studies. Lyon, France: International Agency for Research on Cancer, 1980.
35. Cologne JB, Shibata Y. Optimal case-control matching in practice. Epidemiology 1995;6:271-275.
36. Cologne J, Langholz B. Selecting controls for assessing interaction in nested case-control studies. J Epidemiol 2003;13:193-202.
37. Cologne JB, Tokuoka S, Beebe GW, Fukuhara T, Mabuchi K. Effects of radiation on incidence of primary liver cancer among atomic bomb survivors. Radiat Res 1999;152:364-373.
38. Belsky JL, King RA, Ishimaru T, Hamilton HB, Nakahara Y. Hepatitis-associated antigen in atomic bomb survivors and nonexposed control subjects: seroepidemiologic survey in a fixed cohort. J Infect Dis 1973;128:1-6.
39. IARC. IARC Monographs on the evaluation of the carcinogenic risks to humans. Volume 83: tobacco smoke and involuntary smoking. Lyon, France: IARC; 2004.
40. Yu MC, Yuan JM. Environmental factors and risk for hepatocellular carcinoma. Gastroenterology 2004;127:S72-8.
41. Andersson M. Long-term effects of internally deposited alpha-particle emitting radionuclides. Epidemiological, pathological and molecular-biological studies of Danish Thorotrast-administered patients and their offspring. Dan Med Bull 1997;44:169-190.
42. Baxter PJ, Langlands AO, Anthony PP, Macsween RN, Scheuer PJ. Angiosarcoma of the liver: a marker tumour for the late effects of Thorotrast in Great Britain. Br J Cancer 1980;41:446-453.
43. Sharp GB. The relationship between internally deposited alpha-particle radiation and subsite-specific liver cancer and liver cirrhosis: an analysis of published data. J Radiat Res 2002;43:371-380.
44. Iwamoto KS, Mizuno T, Tokuoka S, Mabuchi K, Seyama T. Frequency of p53 mutations in hepatocellular carcinomas from atomic bomb survivors. J Natl Cancer Inst 1998;90:1167-1168.
45. Nakamura S, Tanaka IB 3rd, Tanaka S, Nakaya K, Sakata N, Oghiso Y. Adiposity in female B6C3F1 mice continuously irradiated with low-dose-rate gamma rays. Radiat Res 2010;173:333-341.
46. Bullock RE, Zaitoun AM, Aithal GP, Ryder SD, Beckingham IJ, Lobo DN. Association of non-alcoholic steatohepatitis without significant fibrosis with hepatocellular carcinoma. J Hepatol 2004;41:685-690.
47. Akahoshi M, Amasaki Y, Soda M, Hida A, Imaizumi M, Nakashima E, et al. Effects of radiation on fatty liver and metabolic coronary risk factors among atomic bomb survivors in Nagasaki. Hypertens Res 2003;26:965-970.

BRIEF REPORT

Effects of Hepatitis B Virus Infection on the Interferon Response in Immunodeficient Human Hepatocyte Chimeric Mice

Masataka Tsuge,[1,2,3] Shoichi Takahashi,[1,3] Nobuhiko Hiraga,[1,3] Yoshifumi Fujimoto,[1,4] Yizhou Zhang,[1,3] Fukiko Mitsui,[1,3] Hiromi Abe,[1,4] Tomokazu Kawaoka,[1,3] Michio Imamura,[1,3] Hidenori Ochi,[1,3,4] C. Nelson Hayes,[1,3] and Kazuaki Chayama[1,3,4]

[1]Department of Medicine and Molecular Science, Division of Frontier Medical Science, Programs for Biomedical Research, Graduate School of Biomedical Sciences, and [2]Live Science Division, Natural Science Center for Basic Research and Development, and [3]Liver Research Project Center, Hiroshima University; [4]Laboratory for Liver Diseases, the RIKEN Center for Genomic Medicine, Hiroshima, Japan

Complementary DNA microarray analysis of human livers cannot exclude the influence of the immunological response. In this study, complementary DNA microarray analysis was performed under immunodeficient conditions with human hepatocyte chimeric mice, and gene expression profiles were analyzed by hepatitis B virus (HBV) infection and/or interferon treatment. The expression levels of 183 of 525 genes upregulated by interferon treatment were significantly suppressed in response to HBV infection. Suppressed genes were statistically significantly associated with the interferon signaling pathway and pattern recognition receptors in the bacteria/virus recognition pathway ($P = 1.0 \times 10^{-8}$ and $P = 1.2 \times 10^{-8}$, respectively). HBV infection attenuated virus recognition and interferon response in hepatocytes, which facilitated HBV escape from innate immunity.

Chronic hepatitis B virus (HBV) infection is associated with the development of virus-related liver diseases, including chronic hepatitis, liver cirrhosis, and hepatocellular carcinoma. Interferon α (IFN-α) has been used for the treatment of chronic hepatitis B, and many large clinical trials and meta-analyses have demonstrated the effectiveness of interferon [1–3]. However, the effect of IFN-α therapy is unsatisfactory, and the molecular basis for tolerance to IFN-α is not clearly defined.

DNA microarray technology has enabled genome-wide analysis of gene transcript levels with the use of clinical tissues and animal models, which has yielded insights into the molecular features of several liver diseases [4–6]. However, it has been difficult to determine whether the changes in gene expression were caused by viral interference or by the human immune response, because all of these studies that used clinical and experimental samples were analyzed under the influence of adaptive immune responses. Recently, Mercer and colleagues developed a human hepatocyte chimeric mouse model [7]. These mice were derived from severe combined immunodeficiency (SCID) mice, which are severely immunocompromised, and the mouse liver cells were extensively replaced with human hepatocytes [7, 8]. With the use of this chimeric mouse model, in which HBV can continuously infect human hepatocytes, the effect of drugs and the response of viral infection can be analyzed in human hepatocytes under immunodeficient conditions [9]. In this study, we performed microarray analysis with human hepatocyte chimeric mouse livers to assess the direct impacts of HBV infection and IFN treatments on gene expression profiles. We successfully demonstrated that HBV infection attenuated the expression of IFN-stimulating genes under immunodeficient conditions, which suggests that HBV proteins might afford escape mechanisms from cellular innate immunity.

METHODS

A serum sample was obtained from a HBV carrier after obtaining written informed consent for the donation and evaluation of the blood sample. The inoculum was positive for Hepatitis B surface and Hepatitis B e antigens, with slightly elevated levels of serum alanine aminotransferase and high-level viremia (HBV DNA load, 7.1 log copies/mL). The studied patient was infected with HBV genotype C. The experimental protocol conformed to the ethical guidelines of the Declaration of Helsinki and was approved by the Hiroshima University Hospital ethical committee (approval ID: D08-9).

The $uPA^{+/+}/SCID^{+/+}$ mice were prepared and the human hepatocytes were transplanted as described elsewhere [8]. The experiments were performed in accordance with the guidelines of the local committee for animal experiments at Hiroshima University.

Sixteen chimeric mice, in which >90% of the liver tissue was replaced with human hepatocytes, were divided into

Received 8 December 2010; accepted 2 March 2011.
Potential conflicts of interest: none reported.
Correspondence: Kazuaki Chayama, MD, PhD, Department of Medical and Molecular Science, Division of Frontier Medical Science, Programs for Biomedical Research, Graduate School of Biomedical Science, Hiroshima University, 1-2-3 Kasumi, Minami-ku, Hiroshima 734-8551, Japan (chayama@hiroshima-u.ac.jp).

The Journal of Infectious Diseases 2011;204:224–8

0022-1899 (print)/1537-6613 (online)/2011/2042-0010$14.00
DOI: 10.1093/infdis/jir247

4 experimental groups. Group A contained 4 mice that were neither infected with HBV nor treated with IFN. Group B consisted of 3 mice that were treated with IFN-α for 6 h (7,000 IU per gram of body weight) just before being humanely killed but were not infected with HBV. Mice in groups C and D were inoculated via the mouse tail vein with human serum containing 6×10^6 copies of HBV. After inoculation, we collected mouse serum samples every 2 weeks and analyzed HBV DNA titers by real-time polymerase chain reaction (PCR) and human albumin levels by means of a human albumin enzyme-linked immunosorbent assay quantitation kit (Bethyl Laboratories), as described elsewhere [9]. Virus and human albumin titer levels are shown in Supplementary data 1. All 9 mice developed measurable viremia 4 weeks after inoculation. Eight weeks after inoculation, 4 of the 9 infected mice (group C) were humanely killed without IFN treatment and the remaining 5 mice (group D) were humanely killed after 6 h of IFN-α treatment (7,000 IU per gram of body weight). The mice were infected, had serum samples extracted, and were killed humanely under ether anesthesia, as described elsewhere [8].

All 16 chimeric mice were killed humanely, and human hepatocytes were finely dissected from the mouse livers and stored in liquid nitrogen after submerging in RNA later solution (Applied Biosystems). Total RNA was extracted with TRIzol reagent (Invitrogen) and labeled with cyanine 3 by use of a low RNA input linear amplification kit (Agilent Technologies) after amplification. Cyanine-3–labeled complimentary RNA was hybridized to a 44-K whole human genome oligo microarray (Agilent). Detailed protocols are described in Supplementary data 2.

Gene expression profiles were analyzed using GeneSpring GX software (version 10.0.2; Tomy Digital Biology). The detailed protocol is described in Supplementary data table 3. Complete linkage hierarchical clustering analysis was applied using Euclidean distance, and differentially expressed genes were annotated using information from the Gene Ontology (GO) Consortium. Global molecular networks and comparisons of canonical pathways were generated using Ingenuity Pathway Analysis (IPA) software (version 8.6; Ingenuity Systems).

Total RNA was extracted from the implanted human hepatocytes in the mouse livers by use of an RNeasy mini kit (Qiagen) and was reverse transcribed. The selected messenger RNA (mRNA) was quantified by real-time PCR using the 7300 real-time PCR system (Applied Biosystems), and the expression of glyceraldehyde-3-phosphate dehydrogenase served as a control. The amplification protocol and primer sequences are described in Supplementary data 4 and 5.

RESULTS

To analyze the direct effects of IFN in human hepatocytes, we compared the gene expression profiles between groups A (mice without IFN treatment) and B (mice with IFN treatment). Of the 1403 genes that remained after screening with the Welch *T* test, 685 genes showed a >3.0-fold change between groups. Of these 685 genes, 525 genes were up-regulated and the other 160 genes down-regulated by IFN. The top 20 IFN-regulated genes are listed in Supplementary data table 6. GO analysis revealed that 8 (40%) of the top 20 genes that were upregulated with IFN treatment were related to immune response.

To analyze the effect of HBV infection in human hepatocytes, we compared the gene expression profiles between groups A (mice without HBV infection) and C (mice with HBV infection). Among the 1,714 genes hat remained after screening, 373 genes showed a >3.0-fold change between groups. Of these 373 genes, 159 genes were up-regulated and the other 214 genes down-regulated by HBV. The top 20 HBV-regulated genes are listed in Supplementary data table 7. Several oncogenic genes such as growth differentiation factor 15 and glial cell derived neurotrophic factor were included in the top group. Most of the top 20 genes that were downregulated with HBV infection were associated with transcriptional regulation.

To examine whether HBV infection may alter the effect of IFN response in human hepatocytes, we compared gene expression profiles among all groups. As mentioned above, 525 genes were upregulated by >3.0-fold by IFN in the absence of HBV infection. A comparison of groups C (mice with HBV infection but no IFN treatment) and D (mice with both HBV infection and IFN treatment) revealed that 183 (34.9%) of the 525 genes showed statistically significantly reduced IFN response with HBV infection ($P < .01$) (Supplementary data 8A). The top 20 genes in which IFN response was significantly changed by HBV infection are shown in Table 1. The mRNA expression levels of 11 selected genes among the 183 genes with reduced IFN response were also analyzed by real-time PCR, and the reductions in IFN response by HBV infection were verified (Supplementary data 8B). Additionally, we used IPA software to analyze the influence of HBV infection on the IFN response of these 183 genes by means of a pathway-oriented approach. Pathway analysis revealed that several pathways were affected by HBV infection (Table 2). The IFN response was statistically significantly attenuated by HBV infection in the pathways related to IFN signaling and pattern recognition of bacteria and viruses ($P = 1.0 \times 10^{-8}$ and $P = 1.2 \times 10^{-8}$, respectively).

DISCUSSION

Elsewhere we have demonstrated a human hepatocyte chimeric mouse model that can be chronically infected with hepatitis B and C viruses [9–11]. This mouse model facilitates analysis of the effect of viral infection and the response to medication under immunodeficient conditions. In this study, we performed complementary DNA microarray analysis using the chimeric mouse model and obtained gene expression profiles to analyze

Table 1. Genes With Interferon Responsiveness Downregulated by Hepatitis B Virus (HBV) Infection

Gene symbol	GenBank accession no.	Function	Fold change in expression level		*P*
			Without HBV infection	With HBV infection	
ENST00000322831	None	Unknown	4.52	−1.45	4.15×10^{-7}
AA593970	AA593970	EST	9.70	1.61	5.58×10^{-7}
THC2533996	None	Unknown	3.74	−2.50	6.97×10^{-7}
LOC388532	None	Unknown	3.11	−2.48	1.61×10^{-6}
ZNF267	NM_003414	Transcription regulator	7.66	1.79	2.30×10^{-6}
ZNF217	NM_006526	Transcription regulator	3.69	1.03	3.62×10^{-6}
CRSP3	NM_015979	Transcription regulator	7.50	−1.02	4.06×10^{-6}
MGC39372	BC025340	Hypothetical protein	30.92	7.03	5.74×10^{-6}
BF972140	BF972140	EST	16.91	4.71	5.78×10^{-6}
LOC731599	XR_015536	Hypothetical protein	3.17	−4.18	8.58×10^{-6}
LOC645676	AK126559	Hypothetical protein	3.76	1.35	9.13×10^{-6}
THC2650457	None	Unknown	78.07	6.28	1.29×10^{-5}
ZNF24	NM_006965	Transcription regulator	3.69	1.36	1.64×10^{-5}
CCDC68	NM_025214	Unknown	5.88	−2.83	1.89×10^{-5}
SP110	NM_004510	Transcription regulator	5.00	10.77	2.00×10^{-5}
FLJ21272	AK024925	Hypothetical protein	14.70	2.49	3.18×10^{-5}
PLEKHF1	NM_024310	Unknown	6.65	1.84	4.70×10^{-5}
AK026418	AK026418	Unknown	9.50	2.58	5.02×10^{-5}
hCG_1790262	XM_001133847	Unknown	3.13	−2.94	6.25×10^{-5}
CEBPD	NM_005195	Transcription regulator	8.16	1.56	7.03×10^{-5}
FLJ20273	NM_019027	RNA binding	3.37	1.11	7.11×10^{-5}

NOTE. *P* values were analyzed by the Welch *T* test. *CEBPD,* CCAAT/enhancer binding protein (C/EBP) delta; *CCDC68,* coiled-coil domain containing 68; *CRSP3,* mediator complex subunit 23 (*MED23*); EST, expressed sequence tag; *FLJ20273,* RNA binding motif protein 47 (*RBM47*); *PLEKHF1,* pleckstrin homology domain containing, family F (with FYVE domain) member 1; *SP110,* SP110 nuclear body protein; *ZNF24,* zinc finger protein 24; *ZNF217,* zinc finger protein 217; *ZNF267,* zinc finger protein 267.

the direct influence of HBV infection and IFN-α treatment on human hepatocytes.

To avoid contamination with mouse tissue, human hepatocyte chimeric mice, in which liver tissue is largely (>90%) replaced by human hepatocytes, were used in the present study. However, a small amount of mouse-derived cells, such as interstitial cells, bile duct cells, and vascular cells, still remain in the chimeric mouse livers. Because of high homology between the human and mouse genomes, the signals from microarray analyses may be influenced by cross-hybridization with mouse mRNA. It is difficult to produce $uPA^{+/+}/SCID^{+/+}$ mice >10 weeks old without hepatocyte transplantation, and a previous study demonstrated that it is feasible to use microarray analysis in a functional genomics analysis of chimeric mice [12]. Therefore, to compensate for the contamination, the mice in group A, which were neither infected with HBV nor treated with IFN, were used as negative controls.

To analyze the effect of IFN treatment, we compared gene expression profiles between groups A (mice without IFN treatment) and B (mice with IFN treatment); 525 genes with >3.0-fold upregulation following IFN treatment were observed. Among them, chemokine (C-X-C motif) ligand 9, chemokine (C-X-C motif) ligand 10, and chemokine (C-X-C motif) ligand 11, which promote T cell adhesion, were remarkably highly induced with IFN treatment (Supplementary data table 6) [13]. These results suggest that the antiviral effects of IFN might involve not only direct activation of IFN-stimulated proteins such as myxovirus resistance protein A and double strand RNA-dependent protein kinase but also activation of immunity via chemokines.

Second, we compared the profiles between groups A (mice without HBV infection) and C (mice with HBV infection). As shown in Supplementary data table 7, more than half (12) of the top 20 genes upregulated by HBV infection localized to the cell membrane or the extracellular region, but 14 (70%) of the 20 downregulated genes localized to the nucleus. In addition, GO analysis demonstrated that genes related to cell cycle and DNA modification were affected by HBV infection. We speculate that HBV infection promotes cell growth and DNA damage in the hepatocyte nucleus and activates the immune response in the cytoplasm. From the clinical standpoint, some healthy HBV carriers develop hepatocellular carcinoma without chronic hepatitis or cirrhosis. The present results strongly support this observation, showing that most of the affected genes are known to be associated with carcinogenesis.

Clinically, HBV is known to develop tolerance to IFN treatment in patients with chronic hepatitis B, although the mechanism is not clear. We analyzed the IFN response with and

Table 2. Pathway Analysis of 183 Interferon-Induced Genes With Interferon Responsiveness Downregulated by Hepatitis B Virus Infection

Canonical pathways	*P*	Genes
Interferon signaling	1.00×10^{-8}	*IFIT3, SOCS1, IFIT1, MX1, IFNGR1, JAK2, STAT1, TAP1, IRF1*
Role of pattern recognition receptors in recognition of bacteria and viruses	1.20×10^{-8}	*IL12A, OAS2, OAS3*(includes EG:4940), *IFIH1, PIK3R3, TLR4, NOD2, TICAM1, DDX58, CASP1, NOD1, TLR3, RIPK2*
Type 1 diabetes mellitus signaling	2.00×10^{-4}	*SOCS1, IL12A, RIPK1, GAD1, SOCS6, SOCS2, IFNGR1, JAK2, STAT1, IRF1*
Prolactin signaling	2.70×10^{-4}	*PIK3R3, SOCS1, SOCS6, SOCS2, NMI, JAK2, STAT1, IRF1*
TREM1 signaling	3.50×10^{-4}	*TLR4, NOD2, ICAM1, CASP1, JAK2, TLR3, CASP5*
Production of nitric oxide and reactive oxygen species in macrophages	3.90×10^{-4}	*PIK3R3, TLR4, RND3, PPP2R2A, PPM1J, RHOU, IFNGR1, MAP3K8, IRF8, JAK2, STAT1, IRF1*
Pathogenesis of multiple sclerosis	1.10×10^{-3}	*CXCL10, CXCL9, CXCL11*
Activation of IRF by cytosolic pattern recognition receptors	2.60×10^{-3}	*IFIH1, RIPK1, DDX58, STAT1, IFIT2, ISG15*
Dendritic cell maturation	2.60×10^{-3}	*B2M, PIK3R3, TLR4, ICAM1, IL12A, IL1RN, IRF8, JAK2, TLR3, STAT1*
Interleukin 12 signaling and production in macrophages	3.60×10^{-3}	*PIK3R3, TLR4, IL12A, IFNGR1, MAP3K8, IRF8, STAT1, IRF1*
Sphingosine-1-phosphate signaling	3.60×10^{-3}	*PIK3R3, S1PR2, RND3, CASP1, RHOU, CASP4, CASP7, CASP5*
JAK-STAT signaling	4.00×10^{-3}	*PIK3R3, SOCS1, SOCS6, SOCS2, JAK2, STAT1*
Growth hormone signaling	4.70×10^{-3}	*PIK3R3, SOCS1, SOCS6, SOCS2, JAK2, STAT1*
Retinoic acid mediated apoptosis signaling	8.50×10^{-3}	*TNFRSF10B, PARP8, TNFSF10, TIPARP, IRF1*

NOTE. *B2M,* beta-2-microglobulin; *CASP1,* caspase 1, apoptosis-related cysteine peptidase (interleukin 1, beta, convertase); *CASP4,* caspase 4, apoptosis-related cysteine peptidase; *CASP5,* caspase 5, apoptosis-related cysteine peptidase; *CASP7,* caspase 7, apoptosis-related cysteine peptidase; *CXCL9,* chemokine (C-X-C motif) ligand 9; *CXCL10,* chemokine (C-X-C motif) ligand 10; *CXCL11,* chemokine (C-X-C motif) ligand 11; *DDX58,* DEAD (Asp-Glu-Ala-Asp) box polypeptide 58; *GAD1,* glutamate decarboxylase 1 (brain, 67kDa); *ICAM1,* intercellular adhesion molecule 1; *IFIH1,* interferon induced with helicase C domain 1; *IFIT1,* interferon-induced protein with tetratricopeptide repeats 1; *IFIT2,* interferon-induced protein with tetratricopeptide repeats 2; *IFIT3,* interferon-induced protein with tetratricopeptide repeats 3; *IFNGR1,* interferon gamma receptor 1; *IL1RN,* interleukin 1 receptor antagonist; *IL12A,* interleukin 12A (natural killer cell stimulatory factor 1, cytotoxic lymphocyte maturation factor 1, p35); IRF, interferon regulatory factor; *IRF1,* interferon regulatory factor 1; *IRF8,* interferon regulatory factor 8; *ISG15,* ISG15 ubiquitin-like modifier; *JAK2,* Janus kinase 2; *MAP3K8,* mitogen-activated protein kinase kinase kinase 8; *MX1,* myxovirus (influenza virus) resistance 1, interferon-inducible protein p78 (mouse); *NMI,* N-myc (and STAT) interactor; *NOD1,* nucleotide-binding oligomerization domain containing 1; *NOD2,* nucleotide-binding oligomerization domain containing 2; *OAS2,* 2′-5′-oligoadenylate synthetase 2, 69/71kDa; *OAS3,* 2′-5′-oligoadenylate synthetase 3, 100kDa; *PARP8,* poly (ADP-ribose) polymerase family, member 8; *PIK3R3,* phosphoinositide-3-kinase, regulatory subunit 3 (gamma); *PPM1J,* protein phosphatase, Mg2+/Mn2+ dependent, 1J; *PPP2R2A,* protein phosphatase 2, regulatory subunit B, alpha; *RHOU,* ras homolog gene family, member U; *RIPK1,* receptor (TNFRSF)-interacting serine-threonine kinase 1; *RIPK2,* receptor-interacting serine-threonine kinase 2; *RND3,* Rho family GTPase 3; *S1PR2,* sphingosine-1-phosphate receptor 2; *SOCS1,* suppressor of cytokine signaling 1; *SOCS2,* suppressor of cytokine signaling 2; *SOCS6,* suppressor of cytokine signaling 6; *STAT1,* signal transducer and activator of transcription 1, 91kDa; *TAP1,* transporter 1, ATP-binding cassette, sub-family B (MDR/TAP); *TICAM1,* Toll-like receptor adaptor molecule 1; *TIPARP,* TCDD-inducible poly(ADP-ribose) polymerase; *TLR3,* Toll-like receptor 3; *TLR4,* Toll-like receptor 4; *TNFRSF10B,* tumor necrosis factor receptor superfamily, member 10b; *TNFSF10,* tumor necrosis factor (ligand) superfamily, member 10; *TREM1,* triggering receptor expressed on myeloid cells 1.

without HBV infection, focusing on the 525 upregulated genes with IFN treatment and using all obtained gene expression profiles. Interestingly, 61.3% of the extracted genes maintained an IFN response, but in 34.9% of those genes, IFN responses were attenuated by HBV infection (Supplementary data 8A). Genes corresponding to interferon signaling, including suppressor of cytokine signaling 1 (*SOCS1*) and interferon regulatory factor 1, and those corresponding to pattern recognition of bacteria and viruses, including nucleotide-binding oligomerization domain containing 1 (*NOD1*) and receptor-interacting serine-threonine kinase 2 (*RIPK2*), were statistically significantly associated with HBV-mediated attenuation to IFN response ($P = 1.0 \times 10^{-8}$ and $P = 1.2 \times 10^{-8}$, respectively). According to these results, HBV infection significantly up-regulated *SOCS1* expression and reduced the IFN responsiveness of *SOCS1*. Thus, *SOCS1* might support chronic infection of HBV in escaping the effects of innate immunity or IFN therapy. On the other hand, genes involved in recognition of viral infection were also inhibited following HBV infection. Both *NOD1* and *RIPK2* are related to innate and adaptive immune responses [14, 15]. We speculated that inhibition of *NOD1* or *RIPK2* expression facilitates HBV survival. Although further study is needed, these results may have important implications for the mechanisms of viral escape from innate immunity.

In conclusion, we performed complementary DNA microarray analysis using human hepatocyte chimeric mice. With this system, we could analyze the direct effects of IFN treatment and HBV infection without the confounding effects of the lymphocyte immunological response and obtained evidence that HBV infection attenuated the virus recognition and IFN response in

hepatocytes, by which means HBV could evade innate immune detection and response.

Supplementary Data

Supplementary data are available at *The Journal of Infectious Diseases* online.

Funding

This work was supported by the Ministry of Education, Sports, Culture and Technology and the Ministry of Health, Labor and Welfare (Grants-in-Aid for scientific research and development).

Acknowledgments

This work was performed at the Research Center for Molecular Medicine, Faculty of Medicine, Hiroshima University. We thank Mari Shiota, Rie Akiyama, and Ruri Mikami for their excellent technical assistance and Aya Furukawa for clerical assistance. The funders had no role in the study design, data collection and analysis, decision to publish, or preparation of the manuscript.

References

1. Hsu HY, Tsai HY, Wu TC, et al. Interferon-alpha treatment in children and young adults with chronic hepatitis B: a long-term follow-up study in Taiwan. Liver Int **2008**; 28:1288–97.
2. Lin SM, Tai DI, Chien RN, Sheen IS, Chu CM, Liaw YF. Comparison of long-term effects of lymphoblastoid interferon alpha and recombinant interferon alpha-2a therapy in patients with chronic hepatitis B. J Viral Hepat **2004**; 11:349–57.
3. Sung JJ, Tsoi KK, Wong VW, Li KC, Chan HL. Meta-analysis: treatment of hepatitis B infection reduces risk of hepatocellular carcinoma. Aliment Pharmacol Ther **2008**; 28:1067–77.
4. Bigger CB, Brasky KM, Lanford RE. DNA microarray analysis of chimpanzee liver during acute resolving hepatitis C virus infection. J Virol **2001**; 75:7059–66.
5. Honda M, Yamashita T, Ueda T, Takatori H, Nishino R, Kaneko S. Different signaling pathways in the livers of patients with chronic hepatitis B or chronic hepatitis C. Hepatology **2006**; 44:1122–38.
6. Okabe H, Satoh S, Kato T, et al. Genome-wide analysis of gene expression in human hepatocellular carcinomas using cDNA microarray: identification of genes involved in viral carcinogenesis and tumor progression. Cancer Res **2001**; 61:2129–37.
7. Mercer DF, Schiller DE, Elliott JF, et al. Hepatitis C virus replication in mice with chimeric human livers. Nat Med **2001**; 7:927–33.
8. Tateno C, Yoshizane Y, Saito N, et al. Near completely humanized liver in mice shows human-type metabolic responses to drugs. Am J Pathol **2004**; 165:901–12.
9. Tsuge M, Hiraga N, Takaishi H, et al. Infection of human hepatocyte chimeric mouse with genetically engineered hepatitis B virus. Hepatology **2005**; 42:1046–54.
10. Hiraga N, Imamura M, Tsuge M, et al. Infection of human hepatocyte chimeric mouse with genetically engineered hepatitis C virus and its susceptibility to interferon. FEBS Lett **2007**; 581:1983–7.
11. Kimura T, Imamura M, Hiraga N, et al. Establishment of an infectious genotype 1b hepatitis C virus clone in human hepatocyte chimeric mice. J Gen Virol **2008**; 89:2108–13.
12. Walters KA, Joyce MA, Thompson JC, et al. Application of functional genomics to the chimeric mouse model of HCV infection: optimization of microarray protocols and genomics analysis. Virol J **2006**; 3:37.
13. Luster AD, Jhanwar SC, Chaganti RS, Kersey JH, Ravetch JV. Interferon-inducible gene maps to a chromosomal band associated with a (4;11) translocation in acute leukemia cells. Proc Natl Acad Sci U S A **1987**; 84:2868–71.
14. Tong HH, Long JP, Li D, DeMaria TF. Alteration of gene expression in human middle ear epithelial cells induced by influenza A virus and its implication for the pathogenesis of otitis media. Microb Pathog **2004**; 37:193–204.
15. Viala J, Chaput C, Boneca IG, et al. Nod1 responds to peptidoglycan delivered by the *Helicobacter pylori* cag pathogenicity island. Nat Immunol **2004**; 5:1166–74.

OPEN ACCESS Freely available online

PLOS ONE

Hepatitis B Virus-Specific miRNAs and Argonaute2 Play a Role in the Viral Life Cycle

C. Nelson Hayes[1,2,3☯], Sakura Akamatsu[1,2,3☯], Masataka Tsuge[3,4], Daiki Miki[1,2,3], Rie Akiyama[1,2,3], Hiromi Abe[1,2], Hidenori Ochi[1,2,3], Nobuhiko Hiraga[1,2,3], Michio Imamura[1,2,3], Shoichi Takahashi[1,2], Hiroshi Aikata[1,3], Tomokazu Kawaoka[1,2,3], Yoshiiku Kawakami[1,2,3], Waka Ohishi[3,5], Kazuaki Chayama[1,2,3]*

1 Department of Gastroenterology and Metabolism, Applied Life Sciences, Institute of Biomedical & Health Sciences, Hiroshima University, Hiroshima, Japan, **2** Laboratory for Digestive Diseases, Center for Genomic Medicine, RIKEN, Hiroshima, Japan, **3** Liver Research Project Center, Hiroshima University, Hiroshima, Japan, **4** Natural Science Center for Basic Research and Development, Hiroshima University, Hiroshima, Japan, **5** Department of Clinical Studies, Radiation Effects Research Foundation, Hiroshima, Japan

Abstract

Disease-specific serum miRNA profiles may serve as biomarkers and might reveal potential new avenues for therapy. An HBV-specific serum miRNA profile associated with HBV surface antigen (HBsAg) particles has recently been reported, and AGO2 and miRNAs have been shown to be stably associated with HBsAg in serum. We identified HBV-associated serum miRNAs using the Toray 3D array system in 10 healthy controls and 10 patients with chronic hepatitis B virus (HBV) infection. 19 selected miRNAs were then measured by quantitative RT-PCR in 248 chronic HBV patients and 22 healthy controls. MiRNA expression in serum versus liver tissue was also compared using biopsy samples. To examine the role of AGO2 during the HBV life cycle, we analyzed intracellular co-localization of AGO2 and HBV core (HBcAg) and surface (HBsAg) antigens using immunocytochemistry and proximity ligation assays in stably transfected HepG2 cells. The effect of AGO2 ablation on viral replication was assessed using siRNA. Several miRNAs, including miR-122, miR-22, and miR-99a, were up-regulated at least 1.5 fold ($P<2E-08$) in serum of HBV-infected patients. AGO2 and HBcAg were found to physically interact and co-localize in the ER and other subcellular compartments. HBs was also found to co-localize with AGO2 and was detected in multiple subcellular compartments. Conversely, HBx localized non-specifically in the nucleus and cytoplasm, and no interaction between AGO2 and HBx was detected. SiRNA ablation of AGO2 suppressed production of HBV DNA and HBs antigen in the supernatant.

Conclusion: These results suggest that AGO2 and HBV-specific miRNAs might play a role in the HBV life cycle.

Citation: Hayes CN, Akamatsu S, Tsuge M, Miki D, Akiyama R, et al. (2012) Hepatitis B Virus-Specific miRNAs and Argonaute2 Play a Role in the Viral Life Cycle. PLoS ONE 7(10): e47490. doi:10.1371/journal.pone.0047490

Editor: Sang-Hoon Ahn, Yonsei University College of Medicine, Republic of Korea

Received July 2, 2012; **Accepted** September 11, 2012; **Published** October 16, 2012

Funding: This work was supported in part by Grants-in-Aid for scientific research and development from the Ministry of Health, Labor and Welfare and Ministry of Education Culture Sports Science and Technology, Government of Japan. The funders had no role in study design, data collection and analysis, decision to publish, or preparation of the manuscript.

Competing Interests: The authors have declared that no competing interests exist.

* E-mail: chayama@hiroshima-u.ac.jp

☯ These authors contributed equally to this work.

Introduction

Hepatitis B virus (HBV) is a partially double-stranded DNA virus in the Hepadnaviridae family [1]. New therapies are urgently needed for the 350 million chronically infected individuals who face a significantly elevated lifetime risk of cirrhosis and hepatocellular carcinoma [2,3]. Recent insight into the role of non-coding RNAs in the liver has highlighted potential applications of microRNAs (miRNAs) in HBV diagnosis and treatment [4,5,6,7,8,9].

MiRNAs are a class of short non-coding RNAs involved in post-transcriptional gene regulation of multiple pathways [10]. In contrast to messenger RNAs, exosome-free extracellular miRNAs may be nuclease-resistant and remain in circulation for long periods of time by being stably bound to AGO2, a component of the RNA-induced silencing complex [11]. The origin and function of these extracellular miRNAs is unclear, but they may serve as biomarkers for liver injury and cancer [4]. Elucidating the function of hepatic miRNAs in HBV infection is important in the development of strategies to eradicate the virus and assess the risk of HCC. A number of miRNAs have been shown to be up- or down-regulated in HBV infection [4,12,13]. Noting that the defective hepatitis delta virus co-opts HBsAg subviral particles for export, Novellino et al. hypothesized that HBsAg subviral particles might also sequester miRNAs from the liver [5]. Using HBsAg immunoprecipitation, they identified a set of liver-specific and immune regulatory AGO2-bound miRNAs associated with HBsAg.

These reports suggest that AGO2 and a specific subset of miRNAs may participate in HBV replication, either as part of a host anti-HBV defense or as viral strategy to exploit or evade the RISC machinery. In this study, we examined serum miRNA expression in chronic HBV and healthy individuals and found a specific subset of miRNAs that are over-expressed in HBV-positive

patients and in which miR-122 was strongly up-regulated. To determine whether components of the miRNA system are associated with other HBV components, we performed subcellular localization experiments with viral proteins and AGO2.

Materials and Methods

Study Subjects

We performed a series of experiments to compare miRNA profiles of healthy and HBV-infected individuals in serum and liver tissue. All patients had chronic hepatitis B and agreed to provide blood samples for a viral hepatitis study. Patient profiles are shown in Table 1. Histopathological diagnosis was made according to the criteria of Desmet et al. [14]. The study protocol conforms to the ethical guidelines of the 1975 Declaration of Helsinki, and all patients provided written informed consent. This study was approved a priori by the ethical committee of Hiroshima University.

miRNA Expression Levels in Serum

miRNA expression in serum samples was measured using the Toray Industries miRNA analysis system, in which serum miRNA samples were hybridized to 3D-Gene human miRNA ver12.1 chips containing 900 miRNAs (Toray Industries, Inc., Tokyo, Japan). MiRNA gene expression data were scaled by global normalization, and differential expression was analyzed using the limma package in the R statistical framework. Serum was collected from 20 patients with high HBV DNA and HBsAg levels and with either high (>42 IU/l) or low (≤42 IU/l) ALT levels. Serum from the 10 low ALT patients was analyzed as a mixture, whereas serum from each of the 10 high ALT patients was analyzed both separately and as a mixture. For comparison with healthy controls we collected separate mixtures of serum from 10 healthy females and 12 healthy males. Serum samples from each healthy female were also measured separately. All healthy controls were negative for HBsAg, HBcAb, and HCV Ab. For comparison with miRNA expression in hepatocytes, miRNA expression was measured in non-tumor biopsy tissue from an HBV-infected patient and compared to non-cancerous liver tissue samples from two patients without HBV or HCV infection.

Table 1. Clinical characteristics of chronic hepatitis B virus patients (n = 248).

Factor	Value
Age	44 (15–76)
Sex (male/female)	169/77
Alanine aminotransferase (IU/l)	56 (10–1867)
Aspartate aminotransferase (IU/l)	43.5 (15–982)
HBV DNA (IU/ml)	6.3 (1.8–9.1)
Liver fibrosis (1/2/3/4)	69/102/46/26
Necroinflammatory activity (0/1/2/3/4)	1/70/127/45/0
γ-glutamyl transpeptidase (IU/l)	43 (9–459)
Alpha-fetoprotein (μg/l)	6.15 (0–9400)
Promthrombin time (s)	93 (0–146)
Albumin (g/dl)	4.4 (0–5.2)
Platelets (x10^4/mm^3)	16.75 (1–36)
HBsAg (IU/l)	2765 (0.05–239000)
HBeAg (−/+)	115/127
HBeAb (−/+)	113/128

Continuous variables are shown as median and range, and categorical variables are shown as counts.
Fibrosis and necroinflammatory activity were scored according to the criteria of Desmet et al. [14].
doi:10.1371/journal.pone.0047490.t001

Quantitative Real-time Polymerase Chain Reaction miRNA Analysis

Using real-time polymerase chain reaction (RT-PCR) we measured the expression of 19 miRNAs in serum from 248 patients with chronic HBV infection and from 10 healthy females and 12 healthy males. Circulating microRNA was extracted from 300 μl of serum samples using the mirVana PARIS Kit (Ambion, Austin, TX) according to the manufacturer's instructions. RNA was eluted in 80 μl of nuclease free water and reverse transcribed using TaqMan MicroRNA Reverse Transcription Kit (Life Technologies Japan, Tokyo, Japan). *Caenorhabditis elegans* miR-238 (cel-miR-238) was spiked to each sample as a control for extraction and amplification steps. The reaction mixture contained 5 μl of RNA solution, 2 μl of 10× reverse transcription buffer, 0.2 μl of 100 mM dNTP mixture, 4 μl of 5× RT primer, 0.25 μl of RNase inhibitor and 7.22 μl of nuclease free water in a total volume of 20 μl. The reaction was performed at 16°C for 30 min followed by 42°C for 30 min. The reaction was terminated by heating the solution at 85°C for 5 min. MiRNAs were amplified using primers and probes provided by Applied Biosystems using TaqMan MicroRNA assays according to the manufacturer's instructions. The reaction mixture contained 12.5 μl of 2× Universal PCR Master Mix, 1.25 μl of 20× TaqMan Assay solution, 1 μl of reverse transcription product and 10.25 μl of nuclease free water in a total volume of 25 μl. Amplification conditions were 95°C for 10 min followed by 50 denaturing cycles for 15 sec at 95°C and annealing and extension for 60 sec at 60°C in an ABI7300 thermal cycler. For the cel-miR-238 assay, a dilution series using chemically synthesized miRNA was used to generate a standard curve that permitted absolute quantification of molecules.

Pathway Analysis

Target genes of differentially expressed miRNAs were predicted based on agreement among three miRNA prediction tools, miRanda, miRBase, and TargetScan. Gene Set Enrichment Analysis (http://www.broadinstitute.org/gsea) was used to identify significantly over-represented gene ontology (GO) terms among the predicted targets.

Plasmid Construction

The construction of wild-type HBV 1.4 genome length, pTRE-HB-wt, was described previously [15]. We used pTRE2 vector without pTet-off vector and doxycycline because a sufficient amount of HBV transcript was produced from internal HBV promoters, and transcription from the pTRE2 promoter is negligible under these conditions. The nucleotide sequence of the HBV genome that we cloned into plasmids pTRE-HB-wt was deposited into GenBank under accession number AB206817.

Cell Culture

HepG2 cells, derived from a human hepatoma cell line, were grown in Dulbecco's modified Eagle's medium (DMEM) supplemented with 10% (v/v) fetal bovine serum at 37°C and under 5% CO_2. For the production of stably transfected cell lines, HepG2 cells were transfected with 20μg of the plasmid pTRE-HB-wt by calcium precipitation and the transfected cells were selected with

400μg/ml hygromycin-included DMEM. Sixty colonies were isolated, and clones that were positive for both HBs and HBe antigens were selected. Finally, one cell line named T23 was selected and used for further experiments. T23 cells continuously produced more than 6 log copies/ml of HBV DNA in supernatant over more than 12 months (data not shown).

Immunocytochemistry

Co-localization between AGO2 and several HBV proteins (HBc, HBs, and HBx) was analyzed using immunocytochemistry, followed by cellular localization assays using antibodies targeting various sub-cellular compartments. HepG2 or T23 cells were seeded in 2-well chamber plates and harvested 48 hours after seeding. The cells were washed with PBS and fixed with 4% (v/v) paraformaldehyde. After fixation, the cells were stained with several primary antibodies (Table S1). The bound antibodies were detected with an Alexa 488-conjugated antibody against rabbit IgG (1:2000) or Alexa 568-conjugated antibody against mouse IgG (1:2000), respectively (Molecular Probes, Eugene, OR). Nuclei were counterstained with 6-diamidino-2-phenylindole (DAPI) (Vector laboratories, Burlingame, CA). The stained cells were examined with a Fluoview FV10i microscope (Olympus, Tokyo, Japan).

In situ Proximity Ligation Assay

We used proximity ligation assays (PLA) to determine whether AGO2 and HBc physically interact. PLA is a recent method to detect protein-protein interactions using protein-DNA conjugates that can be detected using fluorescence microscopy [16]. PLA improves on traditional immunoassays by directly detecting even weak or transient protein interactions [16]. HepG2 and T23 cells were seeded in 2-well chamber plates and harvested 48 hours after seeding. The cells were washed with PBS and fixed with 4% (v/v) paraformaldehyde. After fixation, the cells were stained with primary antibodies. The primary antibodies used are listed in Table S1. After overnight incubation with primary antibody at 4°C, PLA was performed using Duolink II PLA probe anti-rabbit plus and anti-mouse minus and Duolink II Detection Reagents Orange (Olink, Uppsala, Sweden) following the manufacturer's protocol. Nuclei were counterstained with DAPI. Imaging was performed using a Fluoview FV10i microscope.

Analysis of Supernatant HBV Production by RNA Interference Against AGO2

To investigate the necessity of AGO2 for HBV production, we performed RNA interference assay using T23 cells that are HepG2 cells stably transfected with the plasmid pTRE-HB-wt. We used Silencer Select Pre-designed siRNA small interfering RNA targeting *AGO2* (#s25932, Ambion, Austin, TX) and Silencer Select Negative Control #1 siRNA for control (Ambion). T23 cells were transfected with one of the siRNA oligonucleotides (10 nM) using Lipofectamine RNAiMAX (Invitrogen, Carlsbad, CA) according to the manufacturer's instructions. To examine the knockdown effect of siRNAs against *AGO2* by real-time quantitative RT-PCR, T23 cells transfected with siRNAs were harvested 72 hours after transfection. Total RNA was isolated using the QuickGene RNA cultured cell kit S (Fujifilm, Tokyo, Japan). One μg of each RNA sample was reverse transcribed with the SuperScript VILO cDNA Synthesis kit (Invitrogen). First-strand complementary DNA (cDNA) was amplified with specific primers for the coding sequence of *AGO2*. The primers were as follows: forward, 5′-CCAGCATACTACGCTCACCT-3′; reverse, 5′-CAGAGTGTCTTGGTGAACCTG-3′. We quantified *AGO2* mRNA with EXPRESS SYBR Green ER qPCR Supermix Universal (Invitrogen) according to the manufacturer's instructions. Amplification and detection were performed using the Mx3000P Multiplex quantitative PCR system (Stratagene, La Jolla, CA). Results were normalized to the transcript levels of the housekeeping reference gene glyceraldehyde-3-phosphate dehydrogenase (*GAPDH*). Three to seven days after transfection, the culture media were collected to examine HBV production in supernatant. HBs antigen was measured quantitatively using the Abbott chemiluminescence immunoassay kit (Abbott Japan, Tokyo, Japan). HBV DNA levels were determined by Cobas TaqMan HBV standardized real-time PCR assay (Roche Molecular Systems, Pleasanton, CA). Results are expressed in log10 international units/ml. We also evaluated viability of cells using the Cell Counting kit-8 (Dojindo Laboratories, Kumamoto, Japan) at 3, 5 and 7 days after transfection, according to the manufacturer's instructions. All assays were performed in triplicate, and the results are expressed as mean ± SD.

Statistical Analysis

All analyses were performed using the R statistical package (http://www.r-project.org). Continuous variables are reported using the median and range. Moderated t statistics or Mann Whitney U tests were used to detect significant associations, as appropriate, and P-values were adjusted for multiple testing based on the false discovery rate.

Results

MiRNA Microarray Results

We performed miRNA microarray analysis to identify HBV-associated differences in serum miRNA profiles between 10 chronic HBV patients and 10 healthy controls (Fig. S1). 26 miRNAs with an absolute log fold change greater than 1.5 were found to be significantly (P_{FDR} <0.05) up-regulated in serum of HBV patients, and 8 miRNAs were significantly down-regulated (Table 2). MiR-122, miR-22, and miR-99a levels were the most strongly up-regulated in serum of HBV-infected patients, and levels of miR-575, miR-125a-3p, and miR-4294 were the most down-regulated. We also examined miRNAs associated with presence of HBe antigen or HBe antibody, but no miRNAs were significant following correction for multiple testing (data not shown).

Analysis of Serum Sample Mixtures from HBV-infected Patients and Healthy Controls

In addition to individual serum samples, we also examined 4 pooled serum samples as follows: 10 healthy males, 10 healthy females, 10 HBV patients with low ALT levels, and 10 HBV patients with high ALT levels (Fig. S2). In agreement with results from individual analysis, miR-122 and miR-99 levels were significantly higher in serum from HBV serum samples compared to healthy control samples (Table 2). Corresponding results with a log change greater than 1.5 were found for several other miRNAs, including miR-22, miR-642b, miR-125b (up-regulated) and miR-575 and miR-4294 (down-regulated), but results were not significant following correction for multiple testing in the mixture samples due to the small number of samples compared.

RT-PCR Analysis

Serum levels of 19 miRNAs were analyzed using quantitative RT-PCR analysis of 250 chronic HBV patients and 20 healthy controls. Several miRNAs (miR-122, miR-22, miR-99a, miR-720, miR-125b, and miR-1275) were significantly up-regulated in

Table 2. Top 10 up- or down-regulated serum miRNAs associated with chronic HBV infection.

Sample	Direction	miRNA	logFC	AveExpr	t	P	P_{FDR}
Serum	Up	hsa-miR-122	5.97	9.09	12.84	3.27E−12	3.06E−09
		hsa-miR-99a	2.59	6.20	10.73	2.11E−10	2.19E−08
		hsa-miR-22	2.49	9.55	10.47	2.10E−10	2.19E−08
		hsa-miR-191	2.19	8.42	11.87	1.68E−11	3.93E−09
		hsa-miR-642b	2.03	10.07	9.93	5.92E−10	4.26E−08
		hsa-miR-125b	1.95	5.99	8.72	9.91E−09	4.21E−07
		hsa-miR-486-3p	1.79	9.09	8.01	3.19E−08	9.95E−07
		hsa-miR-378	1.78	5.97	9.94	9.00E−10	6.02E−08
		hsa-miR-320d	1.70	7.19	7.88	4.25E−08	1.21E−06
		hsa-miR-23b	1.69	8.99	7.62	7.64E−08	1.93E−06
	Down	hsa-miR-575	−2.10	8.35	−10.00	5.20E−10	4.05E−08
		hsa-miR-125a-3p	−1.99	7.22	−11.91	1.56E−11	3.93E−09
		hsa-miR-4294	−1.75	11.82	−11.37	4.07E−11	7.63E−09
		hsa-miR-92a-2*	−1.64	11.03	−7.70	6.36E−08	1.75E−06
		hsa-miR-1202	−1.59	8.60	−12.41	6.72E−12	3.14E−09
		hsa-miR-30c-1*	−1.31	6.29	−8.66	1.12E−08	4.35E−07
		hsa-miR-1275	−1.19	9.91	−7.50	1.00E−07	2.35E−06
		hsa-miR-3197	−1.05	11.46	−8.58	9.24E−09	4.21E−07
		hsa-miR-1908	−1.03	13.75	−9.05	3.49E−09	2.04E−07
Mixture	Up	hsa-miR-122	6.80	9.09	20.51	1.09E−06	0.001
		hsa-miR-99a	2.58	6.34	9.32	9.80E−05	0.037
		hsa-miR-22	2.07	8.60	3.16	0.020	0.528
		hsa-miR-125b	2.03	6.29	5.09	0.002	0.264
		hsa-miR-1915*	1.80	8.32	6.24	0.001	0.158
		hsa-miR-3648	1.69	14.16	5.06	0.002	0.264
		hsa-miR-642b	1.64	9.82	4.49	0.004	0.377
		hsa-miR-1288	1.39	6.43	3.56	0.012	0.528
		hsa-miR-325	1.30	4.91	2.87	0.047	0.586
		hsa-miR-486-3p	1.29	8.98	3.87	0.009	0.480
	Down	hsa-miR-575	−1.95	8.43	−6.38	0.001	0.158
		hsa-miR-4294	−1.79	11.95	−5.99	0.001	0.158
		hsa-miR-654-3p	−1.35	5.36	−2.99	0.042	0.569
		hsa-miR-1202	−1.24	8.52	−3.97	0.008	0.480
		hsa-miR-1237	−1.06	7.52	−3.10	0.022	0.531
		hsa-miR-744	−1.03	9.51	−2.91	0.028	0.545

Expression levels were compared using moderated t-statistics, and P-values were corrected for multiple testing using the false discovery rate.
logFC: log2 fold-change between patients with chronic HBV infection relative to healthy individuals.
AveExpr: The average log2 expression level for each miRNA over all samples.
t: moderated t-statistic for patients with chronic HBV infection compared to healthy individuals P for each miRNA.
P: uncorrected P-value for t-test.
P_{FDR}: P-value adjusted for multiple testing based on the false discovery rate.
doi:10.1371/journal.pone.0047490.t002

serum from HBV-infected patients (Table 3). Agreement of microarray and RT-PCR results was strongest for up-regulation of miR-122, miR-22, and miR-125b in serum of HBV patients. To determine whether there is a linear relationship between HBV markers and HBV-associated miRNAs, we analyzed the correlation between HBsAg and 6 up-regulated miRNAs. MiR-122, miR-99a, and miR-125b levels were found to be significantly correlated with HBsAg levels with $R^2>0.5$ (Fig. S3). These three miRNAs were also significantly correlated with HBV DNA titers, with R^2 of about 0.4 (Fig. S4). MiR-122 and miR-22 were significantly but diffusely associated with serum ALT levels ($R^2>0.2$; Fig. S5). To identify miRNAs associated with different phases of HBV infection, we also analyzed the 6 significantly up-regulated miRNAs with respect to the presence of HBe antigen and antibody. MiR-122, miR-99a, miR-720, and miR-125b were each highly significantly elevated in chronic HBV patients who were positive for the HBe antigen (P<4.0E−07; Fig. S6). Similarly, each miRNA was significantly elevated in chronic HBV patients who were negative for the HBe antibody (P<9.1E−05; Fig. S7).

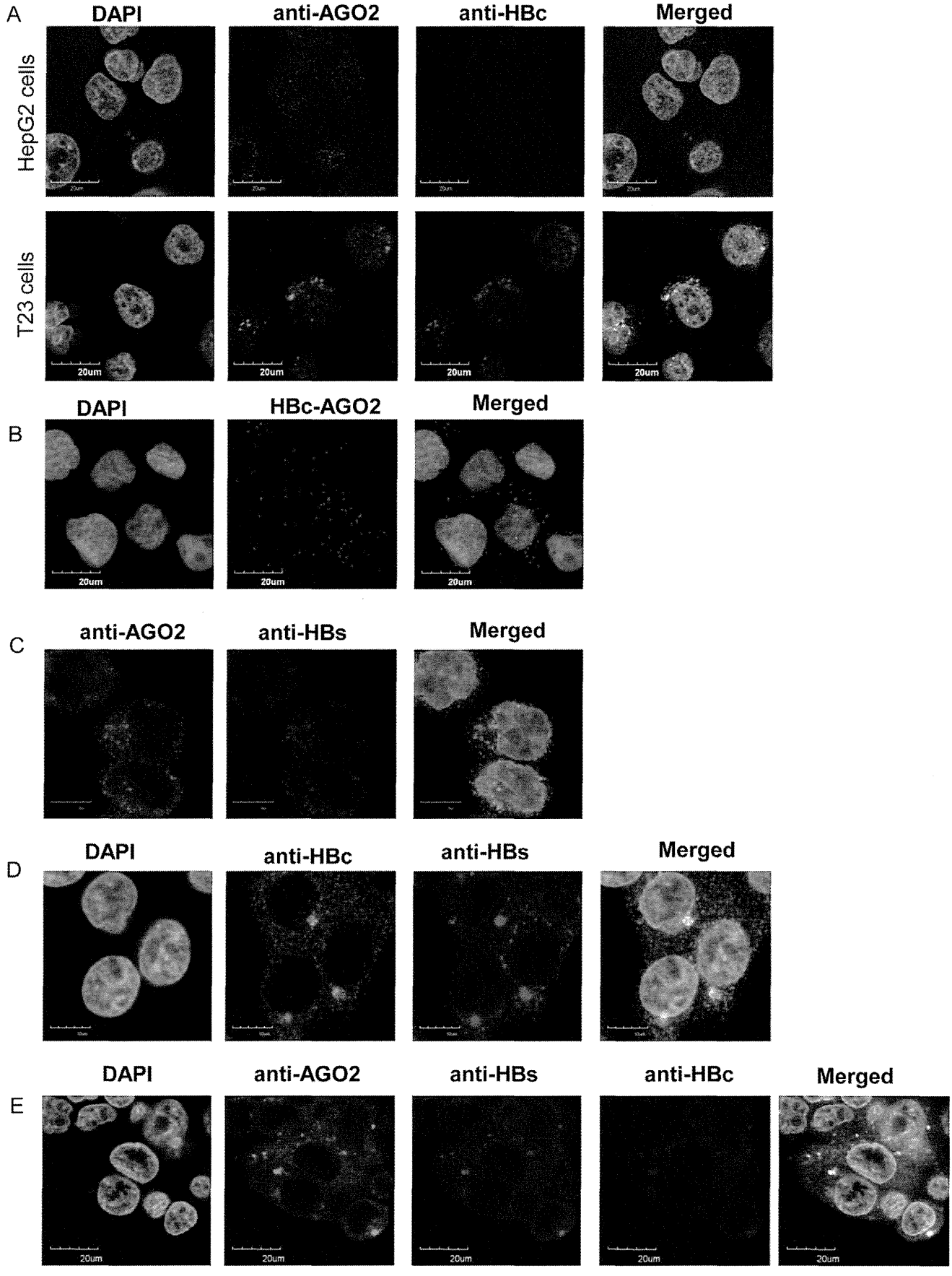
A
DAPI
anti-AGO2
anti-HBc
Merged
HepG2 cells
T23 cells
20um
B
DAPI
HBc-AGO2
Merged
C
anti-AGO2
anti-HBs
Merged
D
DAPI
anti-HBc
anti-HBs
Merged
E
DAPI
anti-AGO2
anti-HBs
anti-HBc
Merged

Figure 1. Co-localization of HBcAg and HBsAg with AGO2 in stably transfected T23 cells. A) Anti-AGO2 and anti-HBc staining overlapped in stably transfected T23 cells, but not in HepG2 control cells, suggesting an interaction between HBc and AGO2. B) HBc-AGO2 was detected in T23 but not HepG2 cells using proximity ligation assays (PLA), suggesting a protein-protein interaction between HBcAg and AGO2. C) Overlap of anti-AGO2 and anti-HBs staining suggests co-localization of HBs and AGO2. D) Anti- HBc, and anti-HBs staining overlapped in T23 cells, which may indicate that HBc and HBs co-localize. E) Overlap of anti-AGO2, anti-HBc, and anti-HBs staining in T23 cells suggests that all three proteins may co-localize.
doi:10.1371/journal.pone.0047490.g001

Pathway Analysis

Predicted gene targets of up-regulated miRNAs were most strongly associated with the GO term PROTEIN_TYROSINE_PHOSPHATASE_ACTIVITY (P = 5.24E−3), and down-regulated miRNAs were associated with the term POSITIVE_REGULATION_OF_JNK_ACTIVITY (P 9.47e−4). Predicted target genes associated with phosphatase activity and dephosphorylation included MTMR3, PTPN18, DUSP5, PTPN2, DUSP2, and PPP1CA.

MiRNA Expression in Liver Biopsy Samples

We compared miRNA expression in non-cancerous liver biopsy samples from a patient with chronic HBV to two uninfected patients (Table S2, Fig. S8). MiRNA levels were highly correlated between liver tissue and serum in all patients (P = <0.001; $R^2 = 0.57$), including the top HBV-associated miRNAs identified by microarray and RT-PCR analysis in this study.

Co-localization of HBcAg and HBsAg with AGO2

Using immunocytochemistry and PLA analysis, we found that HBV core protein and AGO2 co-localized within T23 cells (Fig. 1A–B), suggesting a potential protein-protein interaction between HBcAg and AGO2. AGO2 also co-localized with HBs in T23 cells (Fig. 1C), indicating a potential interaction between HBs and AGO2. Overlap between anti-HBc and anti-HBs staining (Fig. 1D) and between anti-AGO2, anti-HBc, and anti-HBs (Fig. 1E) suggests that these three proteins may co-localize. No overlap was observed between anti-AGO2 and anti-HBx staining in HepG2 cells transfected with HBx expression plasmid (p3FLAG-HBx) nor in control cells, suggesting that HBx does not interact with AGO2 (data not shown).

Subcellular Localization

We also examined HBcAg sub-cellular localization using immunocytochemistry and PLA analysis and found that HBcAg localized to several intracellular compartments, including the ER, autophagosomes, endosomes, and Golgi (Fig. 2). No evidence was found for interaction with mitochondria (data not shown). Using immunocytochemistry, HBsAg was also found to localize diffusely to several intracellular compartments, including the ER, endosomes, autophagosomes, Golgi, mitochondria, processing bodies, multi-vesicular bodies, and the nuclear envelope (Fig. 3). HBx localized non-specifically in the nucleus and cytoplasm, and no sub-cellular location could be ascertained (Fig. S9).

RNA Interference against AGO2

Antisense RNA directed against AGO2 strongly suppressed AGO2 expression (Fig. 4A) and resulted in lower HBV DNA (Fig. 4B) and HBsAg (Fig. 4C) levels in the supernatant. Cell viability was not significantly reduced (Fig. 4D).

Discussion

In this study, we report a set of miRNAs that were up-regulated in serum of HBV infected individuals compared to healthy

Table 3. Quantitative RT-PCR results of selected miRNAs associated in serum of chronic HBV patients.

Factor	Total (n = 270)	HBV (n = 248)	Healthy (n = 22)	P
hsa-miR-122/cel-miR-238	0.1513 (0.0068–2.5)	0.1635 (0.0068–2.5)	0.02074 (0.013–0.04)	1.19E−13
hsa-miR-22/cel-miR-238	0.3 (0.06–1.7)	0.3028 (0.06–1.7)	0.2252 (0.11–0.48)	6.35E−03
hsa-miR-99a/cel-miR-238	0.09121 (0.0046–2.4)	0.102 (0.0086–2.4)	0.0136 (0.0046–0.051)	4.61E−12
hsa-miR-720/cel-miR-238	0.1206 (0.024–3.7)	0.1345 (0.031–3.7)	0.04274 (0.024–0.12)	8.93E−11
hsa-miR-125b/cel-miR-238	0.09732 (0.0066–3.1)	0.1131 (0.0066–3.1)	0.02255 (0.0066–0.05)	1.92E−11
hsa-miR-1275/cel-miR-238	0.4842 (0.099–1.6)	0.5046 (0.099–1.6)	0.4044 (0.24–0.6)	0.010781066
hsa-miR-1826/cel-miR-238	0.5023 (0.14–4.6)	0.5583 (0.26–4.6)	0.33 (0.14–1.4)	7.23E−03
hsa-miR-1308/cel-miR-238	2.831 (1.1–6.9)	2.578 (1.1–6.9)	3.113 (2.3–4.7)	0.223164946
hsa-miR-923/cel-miR-238	3.8 (1.8–9.6)	4.141 (1.8–9.6)	3.01 (2–5)	0.104331611
hsa-miR-1280/cel-miR-238	1.089 (0.36–5)	1.332 (0.6–5)	0.5275 (0.36–0.8)	1.06E−05
hsa-miR-26a/cel-miR-238	1.221 (0.34–3.4)	1.221 (0.34–3.4)	1.231 (0.82–2.4)	0.532171224
hsa-let-7a/cel-miR-238	0.9608 (0.2–2.5)	0.9211 (0.2–2.5)	1.074 (0.71–1.9)	0.235258945
hsa-let-7f/cel-miR-238	1.134 (0.052–2.6)	1.126 (0.052–2.6)	1.143 (0.8–1.7)	0.639411853
hsa-let-7d/cel-miR-238	1.147 (0.35–1.9)	1.106 (0.35–1.8)	1.231 (0.73–1.9)	2.88E−01
hsa-miR-638/cel-miR-238	1.23 (0.3–7)	1.082 (0.3–7)	1.366 (0.68–4)	0.288244047
hsa-miR-1908/cel-miR-238	1.369 (0.45–3.2)	1.357 (0.45–1.9)	1.447 (0.7–3.2)	0.370765019
hsa-miR-34a/cel-miR-238	0.07502 (0.013–1.2)	0.108 (0.026–1.2)	0.02738 (0.013–0.044)	1.41E−05
hsa-miR-886-5p/cel-miR-238	1.627 (0.54–3.6)	1.773 (0.54–3.6)	1.55 (0.97–2.7)	0.478520977

Expression levels were compared using the Mann-Whitney U test.
doi:10.1371/journal.pone.0047490.t003

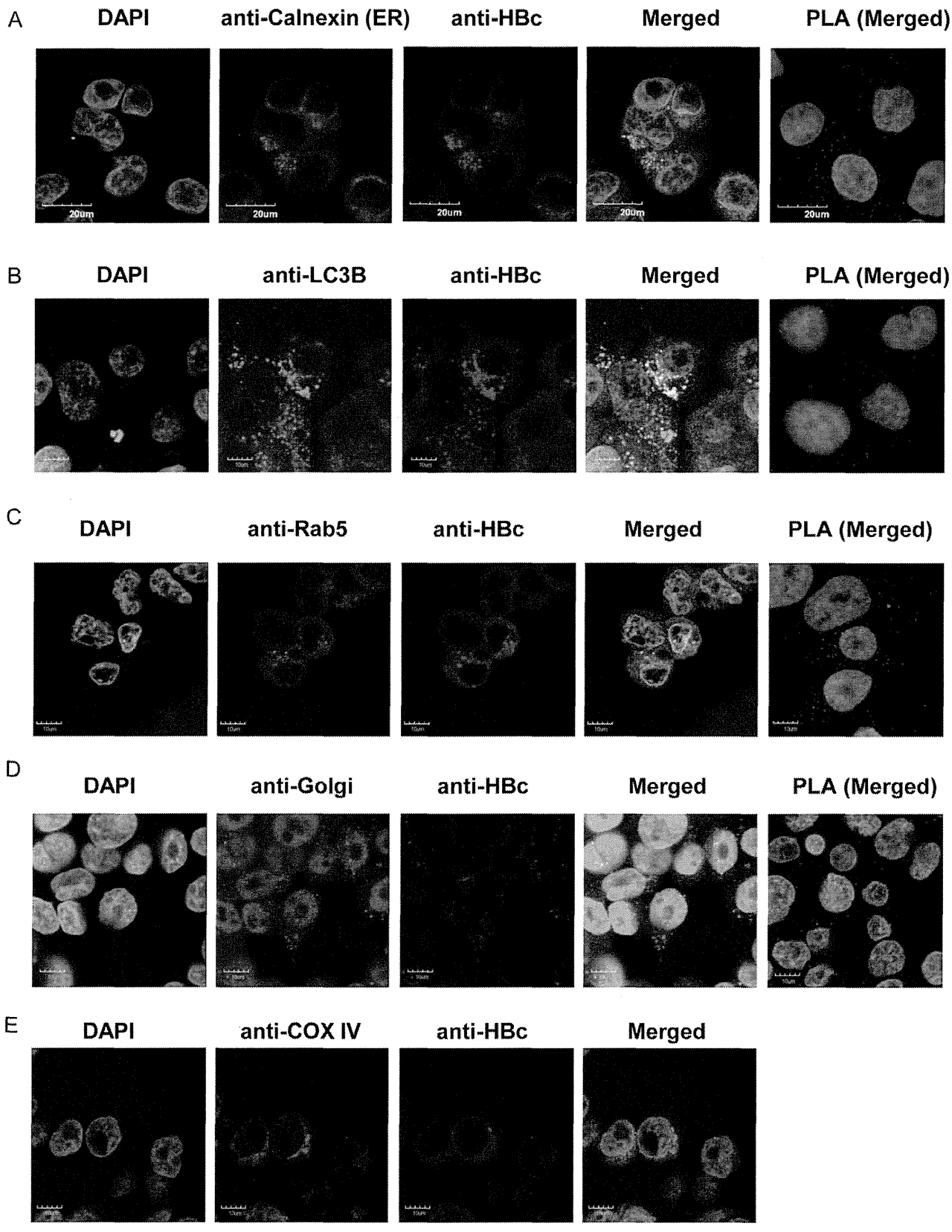

Figure 2. Interactions between HBc and HBs. A) Co-localization of anti-HBc and anti-Calnexin staining by immunocytochemistry and PLA analysis indicate that HBc probably localizes in the ER. Overlap with B) anti-LC3B, C) anti-Rab5, and D) anti-Golgi staining suggests that HBc probably also localizes in autophagosomes, endosomes, and Golgi, respectively. E) However, no overlap was observed with anti-COX IV staining, indicating that HBc probably does not localize at mitochondria.
doi:10.1371/journal.pone.0047490.g002

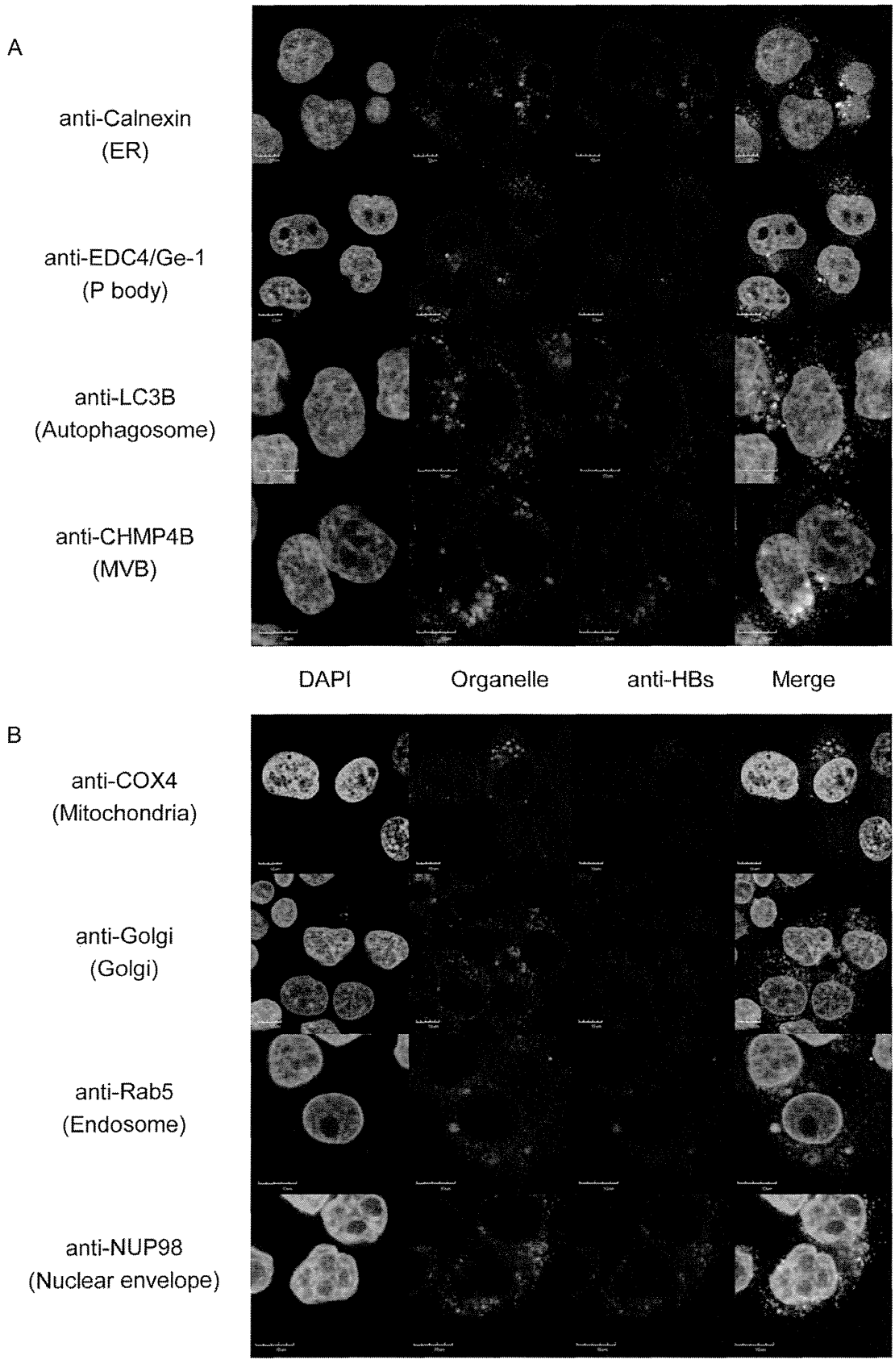

Figure 3. HBsAg localization. A) Co-localization of anti-HBs suggests that HBs localizes in the ER, processing bodies, autophagosomes, and multivesicular bodies, B) and more diffusely in mitochondria, Golgi, endosomes, and at the nuclear envelope.
doi:10.1371/journal.pone.0047490.g003

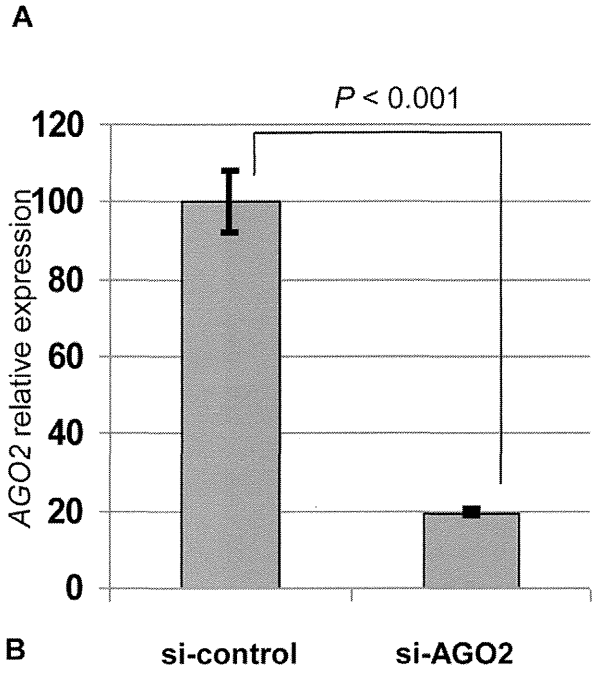
A
P < 0.001
AGO2 relative expression
120
100
80
60
40
20
0
si-control
si-AGO2

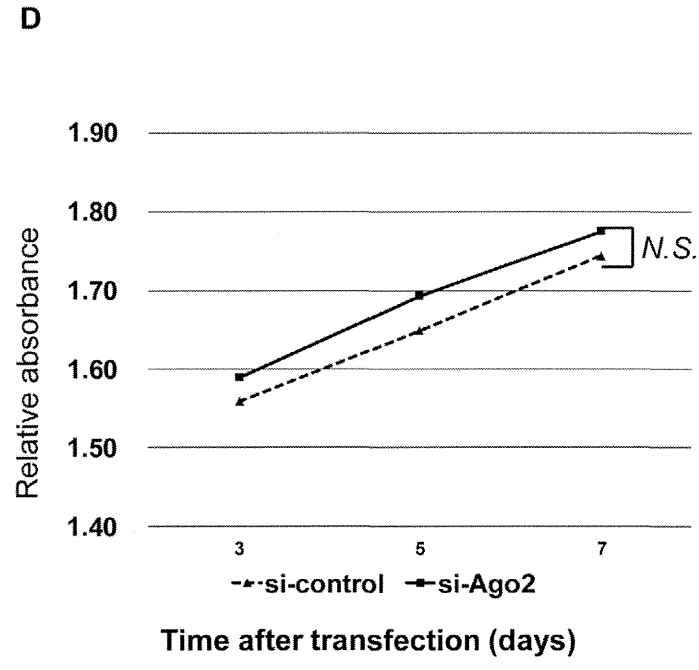
D
Relative absorbance
1.90
1.80
1.70
1.60
1.50
1.40
N.S.
3
5
7
si-control
si-Ago2
Time after transfection (days)

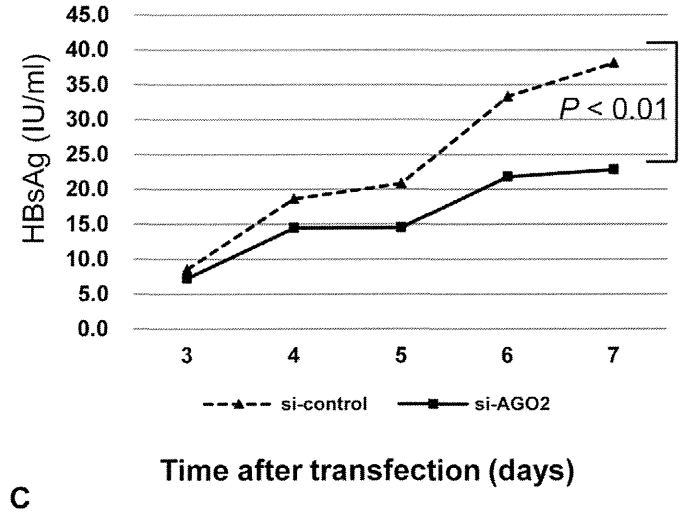
B
HBsAg (IU/ml)
45.0
40.0
35.0
30.0
25.0
20.0
15.0
10.0
5.0
0.0
P < 0.01
3
4
5
6
7
si-control
si-AGO2
Time after transfection (days)

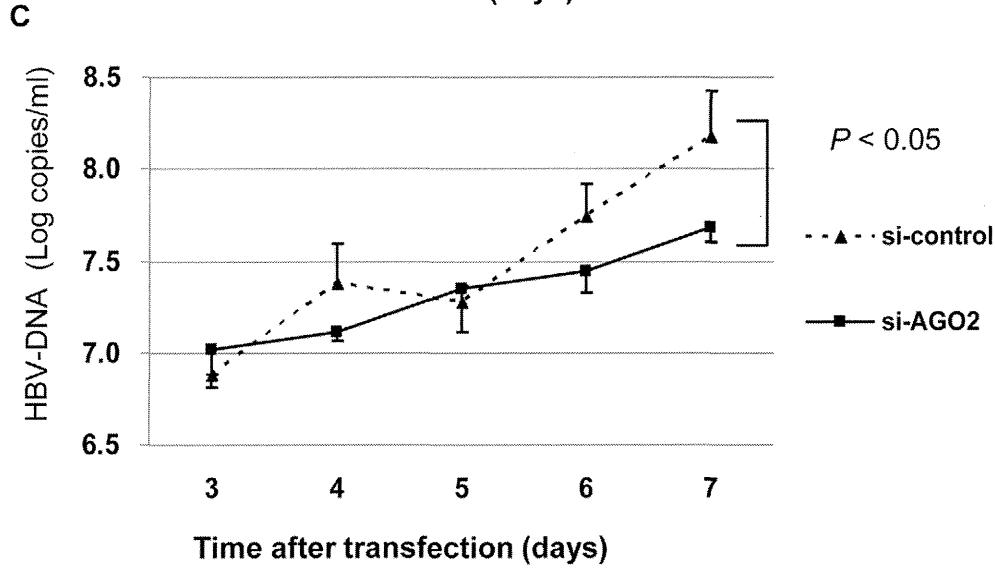
C
HBV-DNA (Log copies/ml)
8.5
8.0
7.5
7.0
6.5
P < 0.05
si-control
si-AGO2
3
4
5
6
7
Time after transfection (days)